


## Hyperon production in quasielastic $\bar{\nu}_\tau$ – nucleon scattering

A. Fatima<sup>✉</sup>, M. Sajjad Athar<sup>✉,\*</sup> and S. K. Singh

*Department of Physics, Aligarh Muslim University, Aligarh-202002, India*

 (Received 5 January 2022; accepted 22 March 2022; published 14 April 2022)

The theoretical results for the total cross sections and polarization components of the  $\tau^+$  lepton produced in the charged current induced  $|\Delta S| = 1$  quasielastic  $\bar{\nu}_\tau - N$  scattering leading to hyperons ( $\Lambda$ ,  $\Sigma$ ) have been presented assuming T invariance. The theoretical uncertainties arising due to the use of different vector, axial-vector, and pseudoscalar form factors as well as the effect of SU(3) symmetry breaking have been studied. We have also presented, for the first time, a comparison of the total cross sections for the production of  $e$ ,  $\mu$ ,  $\tau$  leptons to facilitate the implications of lepton flavor universality in the  $|\Delta S| = 1$  quasielastic reactions induced by the antineutrinos of all flavors i.e.,  $\nu_l$ ;  $l = e, \mu, \tau$ .

DOI: [10.1103/PhysRevD.105.073004](https://doi.org/10.1103/PhysRevD.105.073004)

### I. INTRODUCTION

The  $\tau$  neutrinos ( $\nu_\tau$ ) were experimentally observed for the first time by the DONUT Collaboration [1,2] by observing the  $\tau^-$  leptons produced through the charged current scattering of  $\nu_\tau$  on the nucleons in the reaction,  $\nu_\tau + N \rightarrow \tau^- + X$ , where  $N = n$  or  $p$ , and  $X$  represents hadron(s) in the final state. Since then, a few  $\tau^-$  production events have been observed by the OPERA Collaboration at CERN [3–5] using accelerator neutrinos and by the Super-Kamiokande [6,7], as well as the IceCUBE [8] Collaborations using the atmospheric neutrinos where the  $\nu_\tau$ s are assumed to be produced through the  $\nu_\mu \rightarrow \nu_\tau$  oscillation. Since these experiments have observed very few events of the  $\tau$  lepton production, new experiments for producing larger number of  $\tau$  leptons have been proposed by the SHiP [9–11], DsTau [12], DUNE [13–15], and FASER $\nu$  [16] Collaborations in which the number of  $\tau$  lepton events are expected to reach a few hundred during the running time of 3–5 years of the experiment. The results from these experiments would provide the desired data with reasonable statistics on the total and differential scattering cross sections as well as on the polarization components of the  $\tau$  lepton, which would enable a reliable study of the various aspects and properties of  $\nu_\tau$  and  $\tau$  leptons.

The  $\tau$  lepton production in  $\nu_\tau - N$  scattering has a threshold of 3.5 GeV in the charged current induced quasielastic (CCQE) reactions i.e.,  $\nu_\tau(\bar{\nu}_\tau) + N \rightarrow \tau^-(\tau^+) + N'$  ( $N, N' = n$  or  $p$ ). As the energy increases, the production

of the  $\tau$  leptons is accompanied with the inelastic and deep inelastic production of hadrons. In the energy region of  $\nu_\tau(\bar{\nu}_\tau)$  experiments, where the energy of the produced  $\tau$  lepton is not too large compared to its rest mass  $m_\tau = 1.776$  GeV, the  $\tau$  leptons would not be completely longitudinally polarized, and would also have transverse component of the polarization [17–24]. Moreover, any presence of the polarization component perpendicular to the reaction plane would provide information about the T noninvariance in  $\nu_\tau - N$  interactions [25–28]. The polarization state of the  $\tau$  lepton affects the total and differential cross sections and is, therefore, an important observable in the study of  $\nu_\tau - N$  interactions. Thus, it is highly desirable that a comprehensive study of the  $\tau$  polarization along with the cross sections be made in the quasielastic, inelastic, and deep inelastic reactions induced by  $\nu_\tau$  and  $\bar{\nu}_\tau$  on nucleons in order to understand the  $\nu_\tau - N$  interactions.

In the case of Standard Model (SM) of particle physics, all the leptons interact with each other through the purely leptonic processes and with the quarks through the various semileptonic processes, having the same strength for each leptonic flavor. This is called the lepton flavor universality (LFU) and is an essential feature of the SM.

The validity of LFU has been experimentally studied in the purely leptonic decays of  $\mu, \tau$  leptons as well as in the various semileptonic decays of mesons and baryons. The LFU seems to work quite well in the case of purely leptonic decays of  $\mu$  and  $\tau$  leptons and  $W$  boson [29]. In the case of semileptonic decays of mesons and baryons like  $K, D, D_s^*, \Lambda, \text{ and } \Lambda_c$ , etc., involving quark transitions between medium heavy and light quarks i.e.,  $s \rightarrow u\bar{l}\nu_l, s \rightarrow d\bar{l}\bar{l}, c \rightarrow s\bar{l}\nu_l, c \rightarrow d\bar{l}\nu_l$ , etc., the available experimental results are in agreement with the prediction of SM within statistical uncertainties and no evidence of LFU violation (LFUV) has been reported [30–36]. However, the recent indications of LFUV in semileptonic decays in the heavy quark sector

\*sajathar@gmail.com

*Published by the American Physical Society under the terms of the Creative Commons Attribution 4.0 International license. Further distribution of this work must maintain attribution to the author(s) and the published article's title, journal citation, and DOI. Funded by SCOAP<sup>3</sup>.*

involving transitions like  $b \rightarrow s\bar{l}$  and  $b \rightarrow c\bar{l}\bar{\nu}_l$  at BABAR, LHCb, BESIII, and Belle Collaborations [37–42] have generated great interest in studying the origins of LFUV. Further hints for the LFUV [43,44] have been inferred from the recent measurements of the anomalous magnetic moment ( $g - 2$ ) of the muons, at the Fermilab [45], as well as the anomalies reported in the recent measurements of the Cabibbo angle [46] and production of lepton pairs through the process of  $q\bar{q} \rightarrow \bar{l}l$  ( $l = e$  and  $\mu$ ) in  $pp$  collisions at CERN [47]. In the case of  $b \rightarrow s\bar{l}$  decays, LHCb [39] Collaboration has reported the ratio of the branching fractions in  $l = \mu$  mode to  $l = e$  mode to be  $2.6\sigma$  lower than the SM prediction. While in the case of  $b \rightarrow c\bar{l}\bar{\nu}_l$  decays, all three collaborations [37] have reported the ratio of the branching fraction in  $l = \tau$  mode to  $l = \mu$  mode, which challenge LFU at the level of four standard deviations. This has led to extensive theoretical work in constructing the models of new physics (NP) going beyond the standard model (BSM) to explain these experimental results on LFUV in the  $b$ -quark sector [48–50]. In view of these developments in  $b$ -quark sector, it is natural to apply these theoretical models [48–50] in the medium heavy quark sector involving  $c$  and  $s$  quarks decays like  $c \rightarrow s\bar{l}\bar{\nu}_l$ ,  $c \rightarrow d\bar{l}\bar{\nu}_l$ ,  $s \rightarrow u\bar{l}\bar{\nu}_l$ ,  $s \rightarrow d\bar{l}$  and critically study the LFUV effects and search for them experimentally [51–54]. While these studies are being pursued with some interest, the need for further efforts in this direction has been emphasized recently [34].

Notwithstanding the above efforts in the study of LFUV in the semileptonic decays, there have been very few study of LFUV effects in the (anti)neutrino-nucleus scattering. For example, a comparative study of the quasielastic  $\nu_e(\bar{\nu}_e)$ -nucleon/nucleus and  $\nu_\mu(\bar{\nu}_\mu)$ -nucleon/nucleus scattering and analyzing the differences in the cross sections of these processes arising due to the different nuclear models has been made in Refs. [55–59]. Moreover, the additional effects due to the lepton mass, pseudoscalar form factor, the radiative corrections and second class currents have also been included in Refs. [55,60]. A comparison with the experimental results would give information about the presence or absence of any LFUV effects; however, the present results on the cross sections in the neutrino energy region of a few GeV are not precise enough to conclude about the presence of LFUV effects. Such studies of LFUV effects in the (anti)neutrino scattering with  $\nu_l(\bar{\nu}_l)$ ; ( $l = e, \mu, \tau$ ) in the strange, charm, bottom, and top quark sectors have not been done. With the aim of exploring the presence of such effects in the strangeness sector, we have studied in some detail the quasielastic scattering process of  $\bar{\nu}_l + N \rightarrow l^+ + \Lambda(\Sigma)$ ; ( $l = e, \mu, \tau$ ) corresponding to  $u \rightarrow s$  transition. It should be noted that the production of these hyperons ( $\Lambda, \Sigma^{0,-}$ ) induced by the neutrinos is not allowed due to the  $|\Delta S| = |\Delta Q|$  rule.

In this work, we report on the results of the theoretical calculations within the ambit of the SM with implicit lepton

flavor universality for the total cross section, differential cross section and the  $\tau$  lepton polarization in the reaction  $\bar{\nu}_\tau + p \rightarrow \tau^+ + \Lambda(\Sigma)$ , using various parametrizations for the vector and axial-vector form factors using SU(3) symmetry. The uncertainties in the numerical values of these observables due to the use of different parametrizations of the form factors are discussed. We have also studied the effect of SU(3) symmetry violation using the various weak form factors which have been used to study the SU(3) symmetry violating effects in the semileptonic hyperon decays of  $\Lambda$  and  $\Sigma$  [61,62] and have discussed the uncertainties associated with SU(3) violations. Any deviation of the experimental results on the cross sections and  $\tau$  polarization to be obtained in future will be a signal of LFUV. The results presented here would facilitate the study of LFUV effects in  $\bar{\nu}_l$  ( $l = e, \mu, \tau$ ) induced processes in the strangeness sector corresponding to  $u \rightarrow s$  transition and compliment such LFUV studies in the semileptonic decays of strange particles [63].

In Sec. II, we present the formalism for calculating the differential and total scattering cross sections and using them the polarization observables of the  $\tau$  lepton produced in the quasielastic  $|\Delta S| = 1$  scattering processes have been discussed in Sec. III. In Sec. IV A, we present and discuss the numerical results obtained for the differential cross section and polarization observables of the  $\tau$  lepton and study the dependence of the different parameteric forms of the vector and axial-vector form factors as well as the effect of SU(3) symmetry breaking on these observables. Similar effects are studied in the case of total cross sections and average polarizations in Sec. IV B. Further, we have also studied the lepton flavor universality in the case of  $e - \mu$  and  $e - \mu - \tau$  sectors in the total cross sections and the numerical results are presented for the ratios  $R_1 = \frac{\sigma(\bar{\nu}_\mu + p \rightarrow \mu^+ + \Lambda)}{\sigma(\bar{\nu}_e + p \rightarrow e^+ + \Lambda)}$  and  $R_2 = \frac{2\sigma(\bar{\nu}_\tau + p \rightarrow \tau^+ + \Lambda)}{\sigma(\bar{\nu}_\mu + p \rightarrow \mu^+ + \Lambda) + \sigma(\bar{\nu}_e + p \rightarrow e^+ + \Lambda)}$ , in Sec. IV C. Section V summarizes the results and conclude our findings.

## II. FORMALISM

### A. Matrix element and weak form factors

#### 1. Matrix element

The transition matrix element for the quasielastic hyperon production processes depicted in Fig. 1, given by

$$\bar{\nu}_\tau(k) + N(p) \rightarrow \tau^+(k') + Y(p'), \quad N = p, n; \quad Y = \Lambda, \Sigma^0, \Sigma^-, \quad (1)$$

is written as

$$\mathcal{M} = \frac{G_F}{\sqrt{2}} \sin \theta_c l^\mu J_\mu, \quad (2)$$

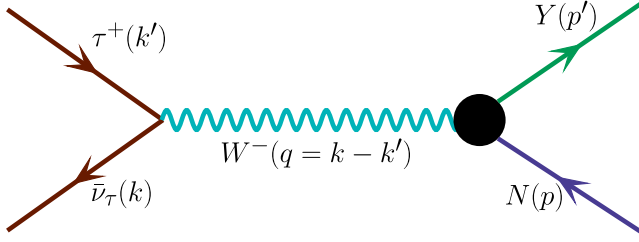


FIG. 1. Feynman diagram for the process  $\bar{\nu}_\tau(k) + N(p) \rightarrow \tau^+(k') + Y(p')$ , where  $N = p, n$ ;  $Y = \Lambda, \Sigma^0, \Sigma^-$  and the quantities in the bracket represent the four-momenta of the corresponding particles.

where the quantities in the brackets of Eq. (1) represent the four-momenta of the respective particles,  $G_F$  is the Fermi

coupling constant and  $\theta_c$  ( $= 13.1^\circ$ ) is the Cabibbo mixing angle. The leptonic current  $l^\mu$  is given by

$$l^\mu = \bar{u}(k')\gamma^\mu(1 + \gamma_5)u(k). \quad (3)$$

The hadronic current  $J_\mu$  is expressed as

$$J_\mu = \bar{u}(p')\Gamma_\mu u(p) \quad (4)$$

with

$$\Gamma_\mu = V_\mu - A_\mu. \quad (5)$$

The vector ( $V_\mu$ ) and the axial-vector ( $A_\mu$ ) currents are given by [25,26]

$$\langle Y(p')|V_\mu|N(p)\rangle = \bar{u}(p')\left[\gamma_\mu f_1^{NY}(Q^2) + i\sigma_{\mu\nu}\frac{q^\nu}{M + M_Y}f_2^{NY}(Q^2) + \frac{2q_\mu}{M + M_Y}f_3^{NY}(Q^2)\right]u(p), \quad (6)$$

$$\langle Y(p')|A_\mu|N(p)\rangle = \bar{u}(p')\left[\gamma_\mu\gamma_5g_1^{NY}(Q^2) + i\sigma_{\mu\nu}\frac{q^\nu}{M + M_Y}\gamma_5g_2^{NY}(Q^2) + \frac{2q_\mu}{M + M_Y}g_3^{NY}(Q^2)\gamma_5\right]u(p), \quad (7)$$

where  $M$  and  $M_Y$  are the masses of the initial nucleon and the final hyperon.  $q(= k - k' = p' - p)$  is the four-momentum transfer with  $Q^2 = -q^2$ ,  $Q^2 \geq 0$ .  $f_1^{NY}(Q^2)$ ,  $f_2^{NY}(Q^2)$ , and  $f_3^{NY}(Q^2)$  are the  $N - Y$  transition vector, weak magnetic and induced scalar form factors and  $g_1^{NY}(Q^2)$ ,  $g_2^{NY}(Q^2)$ , and  $g_3^{NY}(Q^2)$  are the axial-vector, induced tensor (or weak electric), and induced pseudoscalar form factors, respectively.

## 2. Weak transition form factors

The weak vector and axial-vector form factors are determined using the following assumptions, which are consistent with the constraints due to the symmetry properties of the weak hadronic currents [64–66]:

- (a) T invariance implies that all the vector [ $f_i^{NY}(Q^2)$ ;  $i = 1-3$ ] and axial-vector [ $g_i^{NY}(Q^2)$ ;  $i = 1-3$ ] form factors are real.
- (b) The hypothesis that the charged weak vector currents and its conjugate along with the isovector part of the electromagnetic current form an isotriplet implies that the weak vector form factors  $f_1^{NY}(Q^2)$  and  $f_2^{NY}(Q^2)$  are related to the isovector electromagnetic form factors of the nucleon. The hypothesis ensures conservation of vector current (CVC) in the weak sector.
- (c) The hypothesis of CVC of the weak vector currents implies that  $f_3(Q^2) = 0$ .
- (d) The principle of G-invariance implies the second class current form factors to be zero, i.e.,  $f_3^{NY}(Q^2) = 0$  and  $g_2^{NY}(Q^2) = 0$ .

(e) The hypothesis of partially conserved axial-vector current (PCAC) relates the pseudoscalar form factor [ $g_3^{NY}(Q^2)$ ] to the axial-vector form factor [ $g_1^{NY}(Q^2)$ ], through the Goldberger-Treiman (GT) relation.

(f) The assumption of SU(3) symmetry of the weak hadronic currents implies that the vector and axial-vector currents transform as an octet under the SU(3) group of transformations.

The determination of all the weak form factors is based on the symmetry properties discussed above, and the details are given in Ref. [25,26]. The explicit expressions of the vector and axial-vector form factors for the different  $N - Y$  transitions, assuming the SU(3) symmetry are given in Sec. II A 3, while the effects of SU(3) symmetry breaking on these form factors are discussed in Sec. II A 4.

## 3. Form factors with SU(3) symmetry

The weak vector and the axial-vector currents corresponding to the  $\Delta S = 1$  currents whose matrix elements are defined between the initial [ $|N\rangle$ ] and final [ $|Y\rangle$ ] states in Eq. (1) are assumed to belong to the octet representation of the SU(3). Since  $|N\rangle$  and  $|Y\rangle$  also belong to the octet representation under SU(3), each of these form factors are described in terms of the functions  $D(Q^2)$  and  $F(Q^2)$  corresponding to the symmetric (S) and antisymmetric (A) couplings and the SU(3) Clebsch-Gordan coefficients. Explicitly, the form factors can be expressed as (for details, see Ref. [26])

TABLE I. Values of the coefficients  $a$  and  $b$  given in Eqs. (8)–(9).

Transitions	$a$	$b$
$p \rightarrow \Lambda$	$-\sqrt{\frac{3}{2}}$	$-\frac{1}{\sqrt{6}}$
$p \rightarrow \Sigma^0$	$-\frac{1}{\sqrt{2}}$	$\frac{1}{\sqrt{2}}$
$n \rightarrow \Sigma^-$	$-1$	$1$

$$f_i(Q^2) = aF_i^V(Q^2) + bD_i^V(Q^2), \quad (8)$$

$$g_i(Q^2) = aF_i^A(Q^2) + bD_i^A(Q^2), \quad i = 1, 2, 3 \quad (9)$$

The Clebsch-Gordan coefficients  $a$  and  $b$  are calculated for each  $N - Y$  transitions and are given in Table I.

From Table I, we see that the SU(3) symmetry predicts a relation between the vector and axial-vector form factors for the transitions  $p \rightarrow \Sigma^0$  and  $n \rightarrow \Sigma^-$ , which implies that

$$\left[ \frac{d\sigma}{dQ^2} \right]_{p \rightarrow \Sigma^0} = \frac{1}{2} \left[ \frac{d\sigma}{dQ^2} \right]_{n \rightarrow \Sigma^-}, \quad (10)$$

and

$$[P_{L,P}]_{p \rightarrow \Sigma^0} = [P_{L,P}]_{n \rightarrow \Sigma^-}. \quad (11)$$

- (i) *Vector form factors*: In the case of vector form factors, the functions  $D_i^V(Q^2)$  and  $F_i^V(Q^2)$  are determined in terms of the nucleon electromagnetic form factors  $f_i^{n,p}(Q^2)$ ; ( $i = 1, 2$ ), following the same method as discussed above [Eq. (8)] in the case of electromagnetic interactions, i.e.,

$$D_i^V(Q^2) = -\frac{3}{2}f_i^n(Q^2), \quad i = 1, 2 \quad (12)$$

$$F_i^V(Q^2) = f_i^p(Q^2) + \frac{1}{2}f_i^n(Q^2), \quad i = 1, 2. \quad (13)$$

Using the expressions of  $D_i^V(Q^2)$  and  $F_i^V(Q^2)$  obtained above and the values of the coefficients  $a$  and  $b$  from Table I, the vector form factors  $f_{1,2}^{NY}(Q^2)$  are expressed in terms of the nucleon electromagnetic form factors as

$$f_{1,2}^{p\Lambda}(Q^2) = -\sqrt{\frac{3}{2}}f_{1,2}^p(Q^2), \quad (14)$$

$$f_{1,2}^{n\Sigma^-}(Q^2) = -[f_{1,2}^p(Q^2) + 2f_{1,2}^n(Q^2)], \quad (15)$$

$$f_{1,2}^{p\Sigma^0}(Q^2) = -\frac{1}{\sqrt{2}}[f_{1,2}^p(Q^2) + 2f_{1,2}^n(Q^2)]. \quad (16)$$

The electromagnetic nucleon form factors, in turn, are expressed in the terms of the Sachs' electric

$[G_E(Q^2)]$  and magnetic  $[G_M(Q^2)]$  form factors of the nucleons, for which various parametrizations are available in the literature [67–74]. For the numerical calculations, we have used the parametrization given by Bradford *et al.* (BBBA05) [67] unless stated otherwise.

- (ii) *Axial-vector form factors*: We express  $g_1^{NY}(Q^2)$  in terms of  $g_1(Q^2)$  and  $x_1(Q^2)$ , which are defined as

$$g_1(Q^2) = F_1^A(Q^2) + D_1^A(Q^2), \quad (17)$$

$$x_1(Q^2) = \frac{F_1^A(Q^2)}{F_1^A(Q^2) + D_1^A(Q^2)}, \quad (18)$$

where  $F_1^A(Q^2)$  and  $D_1^A(Q^2)$  are the antisymmetric and symmetric couplings of the two octets, determined from the semileptonic decays of hyperons at very low  $Q^2 \approx 0$ . It may be pointed out that there is no information available in the literature, for the  $Q^2$  dependence of these parameters. Therefore, phenomenologically same  $Q^2$  dependence for  $F_1^A$  and  $D_1^A$ , that is the dipole form is assumed, with  $F_1^A(0) = F = 0.463$  and  $D_1^A(0) = D = 0.804$  [75], such that the parameter  $x_1(Q^2)$  becomes a constant, i.e.,  $x_1(Q^2) \approx x_1(0) = 0.364$ .

The explicit expressions of  $g_1^{NY}(Q^2)$  for  $p \rightarrow \Lambda$ ,  $p \rightarrow \Sigma^0$  and  $n \rightarrow \Sigma^-$  are given as

$$g_1^{p\Lambda}(Q^2) = -\frac{1}{\sqrt{6}}(1 + 2x_1)g_1(Q^2), \quad (19)$$

$$g_1^{n\Sigma^-}(Q^2) = (1 - 2x_1)g_1(Q^2), \quad (20)$$

$$g_1^{p\Sigma^0}(Q^2) = \frac{1}{\sqrt{2}}(1 - 2x_1)g_1(Q^2), \quad (21)$$

where

$$g_1(Q^2) = \frac{g_A(0)}{(1 + \frac{Q^2}{M_A^2})^2}, \quad (22)$$

with  $g_A(0) = 1.267$  [75] and  $M_A = 1.026$  GeV [76].

- (iii) *Pseudoscalar form factor*: The contribution of  $g_3^{NY}(Q^2)$  in  $\nu_\tau(\bar{\nu}_\tau) - N$  scattering is significant due to the high value of  $m_\tau$ . In the literature, there exists two parametrizations, given by Marshak *et al.* [64] and by Nambu [77], for the pseudoscalar form factor in the  $\Delta S = 1$  channel. In order to study the effect of the pseudoscalar form factor on the cross section and polarization observables, we have used both the parametrizations. The expression of the pseudoscalar form factor parametrized by Nambu [77] is given as

$$g_3^{NY}(Q^2) = \frac{(M + M_Y)^2}{2(m_K^2 + Q^2)}g_1^{NY}(Q^2), \quad (23)$$

where  $m_K$  is the kaon mass.

In the parametrization of Marshak *et al.* [64], the expression for the pseudoscalar form factor is given as

$$g_3^{NY}(Q^2) = \frac{(M + M_Y)^2 g_1^{NY}(Q^2)(m_K^2 + Q^2) - m_K^2 g_1^{NY}(0)}{2Q^2(m_K^2 + Q^2)}. \quad (24)$$

#### 4. Form factors with SU(3) symmetry breaking effects

In the literature, SU(3) symmetry breaking effects have been studied by various groups [78–86] especially in the

case of semileptonic decays of hyperons. In this work, we have studied the effect of SU(3) symmetry breaking parametrized in the two models by Faessler *et al.* [62] and Schlumpf [61]:

(A) *Faessler et al.* [62]: The main features of the model may be summarized as follows:

- (i) At the leading order, there is no symmetry breaking effect for the vector form factor  $f_1^{NY}(Q^2)$  because of the Ademollo-Gatto theorem [87].
- (ii) In the presence of SU(3) symmetry breaking, the value of  $f_2^{NY}(Q^2)$  is modified from its SU(3) symmetric value  $f_2^{NY}(Q^2)$  to  $\mathcal{F}_2^{NY}(Q^2)$ , as

$$f_2^{p\Lambda}(Q^2) \rightarrow \mathcal{F}_2^{p\Lambda}(Q^2) = f_2^{p\Lambda}(Q^2) - \frac{1}{3\sqrt{6}}[H_1^V(Q^2) - 2H_2^V(Q^2) - 3H_3^V(Q^2) - 6H_4^V(Q^2)], \quad (25)$$

$$f_2^{n\Sigma^-}(Q^2) \rightarrow \mathcal{F}_2^{n\Sigma^-}(Q^2) = f_2^{n\Sigma^-}(Q^2) - \frac{1}{3}[H_1^V(Q^2) + H_3^V(Q^2)], \quad (26)$$

$$f_2^{p\Sigma^0}(Q^2) \rightarrow \mathcal{F}_2^{p\Sigma^0}(Q^2) = f_2^{p\Sigma^0}(Q^2) - \frac{1}{3\sqrt{2}}[H_1^V(Q^2) + H_3^V(Q^2)], \quad (27)$$

where  $f_2^{NY}(Q^2)$  for the different  $N - Y$  transitions are given in Eqs. (14)–(16) and  $H_i^V(Q^2)$ ;  $i = 1-4$  are the SU(3) symmetry breaking terms. Since the symmetry breaking effects, in this model, are studied for the semileptonic decays of hyperons at very low  $Q^2$ , i.e.,  $Q^2 \simeq 0$ , therefore, no information about the  $Q^2$  dependence of  $H_i^V(Q^2)$  is available in the literature. For simplicity, a dipole parametrization is assumed

$$H_i^V(Q^2) = \frac{H_i^V(0)}{(1 + \frac{Q^2}{M_V^2})^2}, \quad i = 1 - 4, \quad (28)$$

where  $M_V = 0.84$  GeV is the vector dipole mass, and the values of the couplings  $H_i^V(0)$  are given in Ref. [62], and are here quoted as

$$\begin{aligned} H_1^V(0) &= -0.246, & H_2^V(0) &= 0.096, \\ H_3^V(0) &= 0.021, & H_4^V(0) &= 0.030. \end{aligned}$$

Similarly, the axial-vector form factor  $g_1^{NY}(Q^2)$ , in the presence of SU(3) symmetry breaking, is modified to  $\mathcal{G}_1^{NY}(Q^2)$  as

$$g_1^{p\Lambda}(Q^2) \rightarrow \mathcal{G}_1^{p\Lambda}(Q^2) = g_1^{p\Lambda}(Q^2) - \frac{1}{3\sqrt{6}}[H_1^A(Q^2) - 2H_2^A(Q^2) - 3H_3^A(Q^2) - 6H_4^A(Q^2)], \quad (29)$$

$$g_1^{n\Sigma^-}(Q^2) \rightarrow \mathcal{G}_1^{n\Sigma^-}(Q^2) = g_1^{n\Sigma^-}(Q^2) - \frac{1}{3}[H_1^A(Q^2) + H_3^A(Q^2)], \quad (30)$$

$$g_1^{p\Sigma^0}(Q^2) \rightarrow \mathcal{G}_1^{p\Sigma^0}(Q^2) = g_1^{p\Sigma^0}(Q^2) + \frac{1}{3\sqrt{2}}[H_1^A(Q^2) + H_3^A(Q^2)], \quad (31)$$

with  $g_1^{NY}(Q^2)$  defined in Eqs. (19)–(21) and a dipole parametrization is assumed for  $H_i^A(Q^2)$  as

$$H_i^A(Q^2) = \frac{H_i^A(0)}{(1 + \frac{Q^2}{M_A^2})^2}, \quad i = 1 - 4 \quad (32)$$

where the couplings  $H_i^A(0)$  are [62]

$$\begin{aligned} H_1^A(0) &= -0.050, & H_2^A(0) &= 0.011, \\ H_3^A(0) &= -0.006, & H_4^A(0) &= 0.037. \end{aligned}$$

- (iii) Since the pseudoscalar form factor is parametrized in terms of the axial-vector form

factor [Eqs. (23) and (24)], therefore, it receives SU(3) symmetry breaking effect via  $g_1^{NY}(Q^2)$ .

- (B) *Schlumpf* [61]: Schlumpf [61] has studied SU(3) symmetry breaking in the hadronic current containing vector ( $f_1$ ) and axial-vector ( $g_1$ ) form factors using the relativistic quark model, and this symmetry breaking in the model originates from the mass difference between  $m_s$  and  $m_{u/d}$  quarks. The modified  $f_1$  and  $g_1$  form factors are given by

$$\begin{aligned} f_1(Q^2) &\rightarrow f'_1(Q^2) = \alpha f_1(Q^2), \\ g_1(Q^2) &\rightarrow g'_1(Q^2) = \beta g_1(Q^2), \end{aligned} \quad (33)$$

where  $\alpha = 0.976, 0.975,$  and  $0.975$ ;  $\beta = 1.072, 1.051,$  and  $1.056$ , respectively for  $p \rightarrow \Lambda, p \rightarrow \Sigma^0$  and  $n \rightarrow \Sigma^-$  transitions. Since the induced pseudo-scalar form factor  $g_3$  is related to the axial-vector form factor  $g_1$ , this modification is also applicable to the terms containing  $g_3$  through Eqs. (23) and (24).

### III. CROSS SECTION AND POLARIZATION OBSERVABLES OF THE FINAL LEPTON

#### A. Cross section

The general expression of the differential cross section for the processes given in Eq. (1), in the laboratory frame, is given by

$$d\sigma = \frac{1}{(2\pi)^2} \frac{1}{4ME_{\bar{\nu}_\tau}} \delta^4(k+p-k'-p') \frac{d^3k' d^3p'}{2E_{k'} 2E_{p'}} \overline{\sum} \sum |\mathcal{M}|^2. \quad (34)$$

Using Eqs. (2)–(4), the transition matrix element squared is obtained as

$$\overline{\sum} \sum |\mathcal{M}|^2 = \frac{G_F^2 \sin^2 \theta_c}{2} \mathcal{J}^{\mu\nu} \mathcal{L}_{\mu\nu}, \quad (35)$$

where the hadronic ( $\mathcal{J}_{\mu\nu}$ ) and the leptonic ( $\mathcal{L}_{\mu\nu}$ ) tensors are obtained using Eqs. (3) and (4) as

$$\mathcal{J}_{\mu\nu} = \overline{\sum} \sum J_\mu J_\nu^\dagger, \quad \mathcal{L}^{\mu\nu} = \overline{\sum} \sum l_\mu l_\nu^\dagger. \quad (36)$$

Following the above definitions, the differential scattering cross section  $d\sigma/dQ^2$  for the processes given in Eq. (1) is written as

$$\frac{d\sigma}{dQ^2} = \frac{G_F^2 \sin^2 \theta_c}{8\pi M^2 E_{\bar{\nu}_\tau}^2} N(Q^2), \quad (37)$$

where  $N(Q^2) = \mathcal{J}^{\mu\nu} \mathcal{L}_{\mu\nu}$  is obtained from the expression given in Appendix A of Ref. [26] with the substitution of  $M' = M_Y$  and  $m_\mu = m_\tau$ .

#### B. Polarization of the final lepton

Using the covariant density matrix formalism, the polarization four-vector ( $\zeta^\tau$ ) of the  $\tau$  lepton produced in the final state in the reactions given in Eq. (1) is written as [88,89]

$$\zeta^\tau = \frac{\text{Tr}[\gamma^\tau \gamma_5 \rho_f(k')]}{\text{Tr}[\rho_f(k')]}, \quad (38)$$

and the spin density matrix for the final lepton  $\rho_f(k')$  is given by

$$\rho_f(k') = \mathcal{J}^{\alpha\beta} \text{Tr}[\Lambda(k') \gamma_\alpha (1 + \gamma_5) \Lambda(k) \tilde{\gamma}_\beta (1 + \tilde{\gamma}_5) \Lambda(k')], \quad (39)$$

with  $\tilde{\gamma}_\alpha = \gamma^0 \gamma_\alpha^\dagger \gamma^0$  and  $\tilde{\gamma}_5 = \gamma^0 \gamma_5^\dagger \gamma^0$ .

Using the following relations

$$\Lambda(k') \gamma^\tau \gamma_5 \Lambda(k) = 2m_\tau \left( g^{\tau\sigma} - \frac{k'^\tau k'^\sigma}{m_\tau^2} \right) \Lambda(k') \gamma_\sigma \gamma_5, \quad (40)$$

and

$$\Lambda(k') \Lambda(k) = 2m_\tau \Lambda(k'), \quad (41)$$

$\zeta^\tau$  defined in Eq. (38) may also be rewritten as

$$\begin{aligned} \zeta^\tau &= \left( g^{\tau\sigma} - \frac{k'^\tau k'^\sigma}{m_\tau^2} \right) \\ &\times \frac{\mathcal{J}^{\alpha\beta} \text{Tr}[\gamma_\sigma \gamma_5 \Lambda(k') \gamma_\alpha (1 + \gamma_5) \Lambda(k) \tilde{\gamma}_\beta (1 + \tilde{\gamma}_5)]}{\mathcal{J}^{\alpha\beta} \text{Tr}[\Lambda(k') \gamma_\alpha (1 + \gamma_5) \Lambda(k) \tilde{\gamma}_\beta (1 + \tilde{\gamma}_5)]}, \end{aligned} \quad (42)$$

where  $m_\tau$  is the mass of the  $\tau$  lepton. In Eq. (42), the denominator is directly related to the differential cross section given in Eq. (37).

With  $\mathcal{J}^{\alpha\beta}$  and  $\mathcal{L}_{\alpha\beta}$  given in Eq. (36), an expression for  $\zeta^\tau$  is obtained. In the laboratory frame where the initial nucleon is at rest, the polarization vector  $\vec{\zeta}$ , assuming T invariance, is calculated to be a function of the three-momenta of incoming antineutrino ( $\vec{k}$ ) and outgoing lepton ( $\vec{k}'$ ), and is given as

$$\vec{\zeta} = [A^l(Q^2) \vec{k} + B^l(Q^2) \vec{k}'], \quad (43)$$

where the expressions of  $A^l(Q^2)$  and  $B^l(Q^2)$  are obtained from the expression given in Appendix B of Ref. [26] with the substitution  $M' = M_Y$  and  $m_\mu = m_\tau$ .

One may expand the polarization vector  $\vec{\zeta}$  along the orthogonal directions,  $\hat{e}_L^l$ ,  $\hat{e}_p^l$ , and  $\hat{e}_T^l$  in the reaction plane

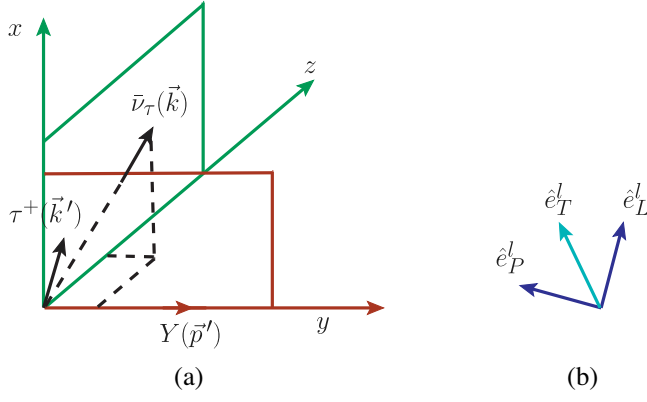


FIG. 2. (a) Momentum and polarization directions of the final lepton produced in the reaction  $\bar{\nu}_\tau(k) + N(p) \rightarrow \tau^+(k') + Y(p')$ . (b)  $\hat{e}_L^l$ ,  $\hat{e}_P^l$ , and  $\hat{e}_T^l$  represent the orthogonal unit vectors corresponding to the longitudinal, perpendicular and transverse directions with respect to the momentum of the final lepton.

corresponding to the longitudinal, perpendicular, and transverse directions of the final lepton ( $l$ ), as depicted in Fig. 2 and defined as

$$\hat{e}_L^l = \frac{\vec{k}'}{|\vec{k}'|}, \quad \hat{e}_P^l = \hat{e}_L^l \times \hat{e}_T^l, \quad \text{where } \hat{e}_T^l = \frac{\vec{k} \times \vec{k}'}{|\vec{k} \times \vec{k}'|}. \quad (44)$$

We then write  $\vec{\zeta}$  as

$$\vec{\zeta} = \zeta_L \hat{e}_L^l + \zeta_P \hat{e}_P^l + \zeta_T \hat{e}_T^l, \quad (45)$$

such that the longitudinal and perpendicular components of the  $\vec{\zeta}$  in the laboratory frame are given by

$$\zeta_L(Q^2) = \vec{\zeta} \cdot \hat{e}_L^l, \quad \zeta_P(Q^2) = \vec{\zeta} \cdot \hat{e}_P^l. \quad (46)$$

From Eq. (46), the longitudinal  $P_L(Q^2)$  and perpendicular  $P_P(Q^2)$  components of the polarization vector defined in the rest frame of the outgoing lepton are given by

$$P_L(Q^2) = \frac{m_\tau}{E_{k'}} \zeta_L(Q^2), \quad P_P(Q^2) = \zeta_P(Q^2), \quad (47)$$

where  $\frac{m_\tau}{E_{k'}}$  is the Lorentz boost factor along  $\vec{k}'$ . Using Eqs. (43), (44), and (46) in Eq. (47), the longitudinal  $P_L(Q^2)$  and perpendicular  $P_P(Q^2)$  components are calculated to be

$$P_L(Q^2) = \frac{m_\tau}{E_{k'}} \frac{A^l(Q^2) \vec{k} \cdot \vec{k}' + B^l(Q^2) |\vec{k}'|^2}{N(Q^2) |\vec{k}'|}, \quad (48)$$

$$P_P(Q^2) = \frac{A^l(Q^2) [|\vec{k}|^2 |\vec{k}'|^2 - (\vec{k} \cdot \vec{k}')^2]}{N(Q^2) |\vec{k}'| |\vec{k} \times \vec{k}'|}, \quad (49)$$

where  $N(Q^2) = \mathcal{J}^{\mu\nu} \mathcal{L}_{\mu\nu}$  is obtained from the expression given in Appendix A of Ref. [26].

## IV. RESULTS AND DISCUSSION

In this section, we present and discuss the results of the differential (Sec. IV A) and total (Sec. IV B) scattering cross sections as well as the polarization observables of the final  $\tau$  lepton produced in the  $|\Delta S| = 1$  quasielastic scattering of  $\bar{\nu}_\tau$  from nucleons. We also present a comparison of the total cross section for the production of  $e$ ,  $\mu$ , and  $\tau$  leptons in the quasielastic scattering of  $\bar{\nu}_e$ ,  $\bar{\nu}_\mu$ , and  $\bar{\nu}_\tau$  to demonstrate the implications of LFU in these processes (Sec. IV C).

### A. Differential scattering cross section and polarization observables

We have used Eqs. (37), (48), and (49), respectively, to numerically evaluate the differential scattering cross section  $d\sigma/dQ^2$ , the longitudinal  $[P_L(Q^2)]$  and the perpendicular  $[P_P(Q^2)]$  components of polarization of  $\tau$  lepton. The Dirac and Pauli form factors  $f_{1,2}^N(Q^2)$ ; ( $N = p, n$ ) are expressed in terms of the electric and magnetic Sachs' form factors, for which the various parametrizations [67–72] available in the literature, have been used. For  $g_1(Q^2)$  a dipole parametrization has been used [Eq. (22)], with the world average value of the axial-dipole mass  $M_A = 1.026$  GeV. For the pseudoscalar form factor  $g_3(Q^2)$ , the parametrizations given by Nambu [77] and Marshak *et al.* [64] have been used. The numerical results of the differential scattering cross section and polarization observables obtained assuming SU(3) symmetry and the results with SU(3) symmetry breaking effects, using the prescriptions of: (i) Faessler *et al.* [62], and (ii) Schlumpf [61], are presented separately for the  $\Lambda$  and  $\Sigma^-$  productions from the nucleons. The results for the  $\Sigma^0$  production can be expressed in terms of the  $\Sigma^-$  production in the SU(3) symmetric limit [Eqs. (10) and (11)] and are not presented separately.

#### 1. $\Lambda$ production

In Fig. 3, we present the results for the  $Q^2$  distribution i.e.,  $\frac{d\sigma}{dQ^2}$ ,  $P_L(Q^2)$  and  $P_P(Q^2)$  vs  $Q^2$  for  $\bar{\nu}_\tau + p \rightarrow \tau^+ + \Lambda$  process at the three different values of energy viz.  $E_{\bar{\nu}_\tau} = 4$  GeV, 5 GeV, and 10 GeV, assuming SU(3) symmetry with  $M_A = 1.026$  GeV and using the different parametrizations of the nucleon vector form factors viz. BBBA05 [67], Alberico [70], Bosted [68], Galster [72], and Kelly [71]. We see that at low  $\bar{\nu}_\tau$  energies, for example at  $E_{\bar{\nu}_\tau} = 4$  GeV, there is considerable dependence of the different parametrizations of the vector form factors on  $\frac{d\sigma}{dQ^2}$ ,  $P_L(Q^2)$ , and  $P_P(Q^2)$  distributions. However, with the increase in  $\bar{\nu}_\tau$  energy, this difference decreases and becomes

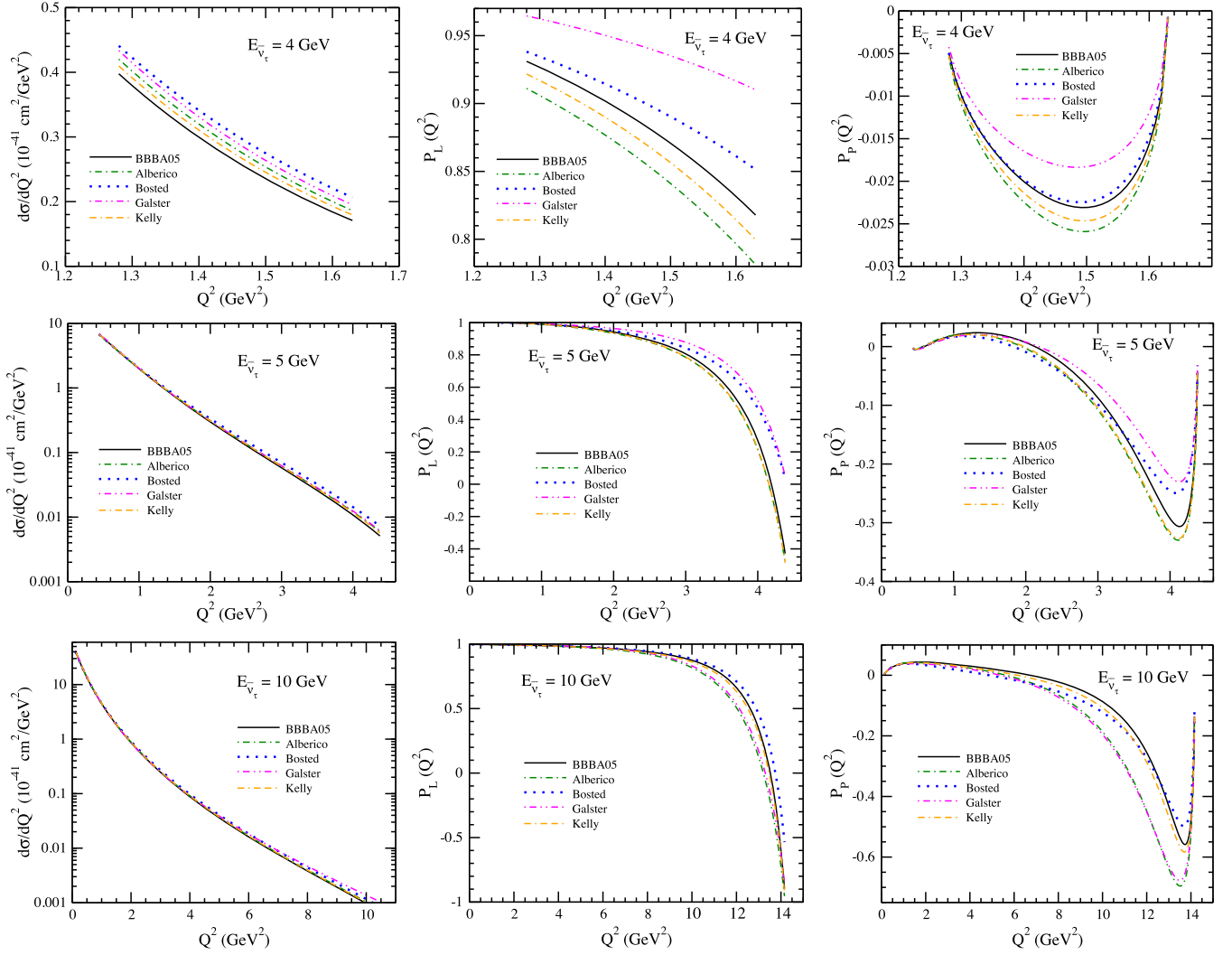


FIG. 3.  $\frac{d\sigma}{dQ^2}$  (left panel),  $P_L(Q^2)$  (middle panel) and  $P_P(Q^2)$  (right panel) versus  $Q^2$  for the process  $\bar{\nu}_\tau + p \rightarrow \tau^+ + \Lambda$  at  $E_{\bar{\nu}_\tau} = 4$  GeV (upper panel), 5 GeV (middle panel) and 10 GeV (lower panel). The calculations have been performed using the SU(3) symmetry with the axial dipole mass  $M_A = 1.026$  GeV and for the different parametrizations of the nucleon vector form factors viz. BBBA05 [67] (solid line), Alberico *et al.* [70] (dashed-dotted line), Bosted [68] (dotted line), Galster *et al.* [72] (double-dotted-dashed line), and Kelly [71] (double-dashed-dotted line).

almost negligible at higher energies, like at  $E_{\bar{\nu}_\tau} = 10$  GeV, especially for  $\frac{d\sigma}{dQ^2}$  and  $P_L(Q^2)$  distributions.

To study the effect of the variation in  $M_A$  (in the range 0.9 GeV–1.3 GeV) on the differential cross section and polarization observables, we present in Fig. 4, the results for  $\frac{d\sigma}{dQ^2}$ ,  $P_L(Q^2)$  and  $P_P(Q^2)$  distributions at  $E_{\bar{\nu}_\tau} = 4$  GeV, 5 GeV, and 10 GeV. We find that at low  $\bar{\nu}_\tau$  energies, there is a significant dependence of these distributions on the choice of  $M_A$ . With the increase in  $\bar{\nu}_\tau$  energy, this dependence on the variation in  $M_A$  decreases, especially for  $\frac{d\sigma}{dQ^2}$  and to some extent for  $P_L(Q^2)$  but not for  $P_P(Q^2)$  distribution. Moreover, it is important to point out that in the case of  $\bar{\nu}_\tau + p \rightarrow \tau^+ + \Lambda$  reaction, with the increase in  $M_A$ ,  $\frac{d\sigma}{dQ^2}$  decreases (0.9 GeV to 1.1 GeV), but with the

further increase in  $M_A$  (1.1 GeV to 1.3 GeV),  $\frac{d\sigma}{dQ^2}$  increases, which is not generally the case in  $\nu_l + n \rightarrow l^- + p$ ; ( $l = e, \mu, \tau$ ) scattering. Moreover, in the case of  $\bar{\nu}_l + p \rightarrow l^+ + n$ , we have observed that with the increase in  $M_A$ ,  $\frac{d\sigma}{dQ^2}$  decreases (from 0.9 GeV to 1.1 GeV) and with further increase in  $M_A = 1.2$  GeV,  $\frac{d\sigma}{dQ^2}$  increases [17]. In the present work, for  $\Lambda$  production we observe a similar trend as in the case of the  $\bar{\nu}_\tau$  induced CCQE reaction [17]. In the  $\bar{\nu}_\tau$  induced reactions because of the production of massive  $\tau$  lepton in the final state, the pseudoscalar form factor becomes significant. The variation in  $\frac{d\sigma}{dQ^2}$  observed in Fig. 4 arises due to interference of the pseudoscalar form factor with axial-vector and vector form factors.



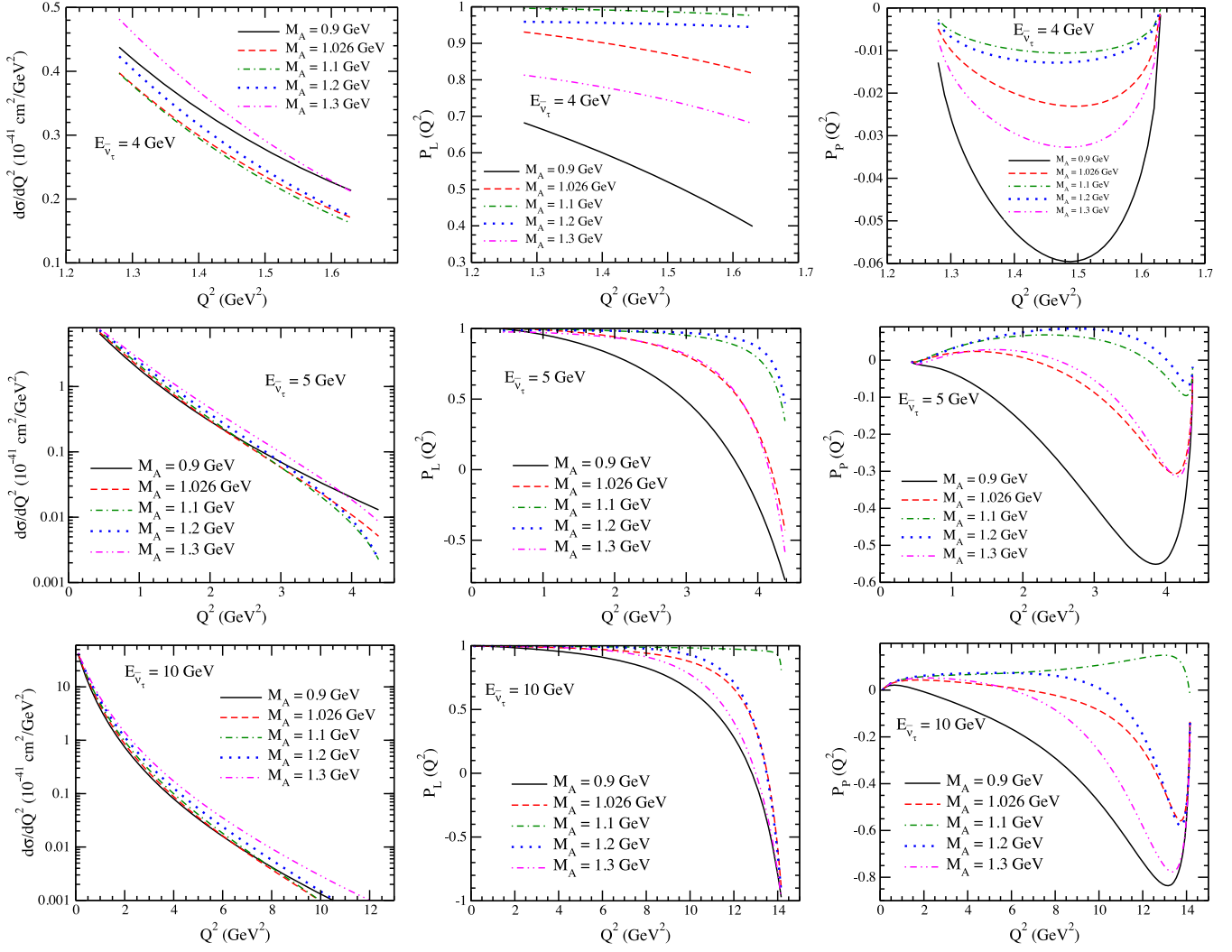


FIG. 4.  $\frac{d\sigma}{dQ^2}$  (left panel),  $P_L(Q^2)$  (middle panel) and  $P_P(Q^2)$  (right panel) versus  $Q^2$  for the process  $\bar{\nu}_\tau + p \rightarrow \tau^+ + \Lambda$  at  $E_{\bar{\nu}_\tau} = 4$  GeV (upper panel), 5 GeV (middle panel) and 10 GeV (lower panel). The calculations have been performed using the SU(3) symmetry with the electric and magnetic Sachs form factors parametrized by Bradford *et al.* [67] and for the axial-vector form factor, the different values of  $M_A$  have been used viz.  $M_A = 0.9$  GeV (solid line), 1.026 GeV (dashed line), 1.1 GeV (dashed-dotted line), 1.2 GeV (dotted line), and 1.3 GeV (double-dotted-dashed line).

To see the dependence of  $\frac{d\sigma}{dQ^2}$ ,  $P_L(Q^2)$  and  $P_P(Q^2)$  on the pseudoscalar form factor  $g_3^{NY}(Q^2)$ , we have used the two parametrizations of  $g_3^{NY}(Q^2)$  given in Eqs. (23) by Nambu [77], and (24) by Marshak *et al.* [64], and show the numerical results in Fig. 5. It may be observed that at low  $\bar{\nu}_\tau$  energies, there is a large dependence on the choice of  $g_3^{NY}(Q^2)$ . While with the increase in  $E_{\bar{\nu}_\tau}$ , this dependence on the choice of  $g_3^{NY}(Q^2)$  becomes almost negligible for the  $\frac{d\sigma}{dQ^2}$  distribution, whereas for  $P_L(Q^2)$  and  $P_P(Q^2)$  distributions, they are found to be quite significant even for the higher values of  $E_{\bar{\nu}_\tau}$ , say  $E_{\bar{\nu}_\tau} = 10$  GeV.

In Fig. 6 we present the results for  $\frac{d\sigma}{dQ^2}$ ,  $P_L(Q^2)$  and  $P_P(Q^2)$  vs  $Q^2$  at  $E_{\bar{\nu}_\tau} = 4$  GeV, 5 GeV, and 10 GeV, when the SU(3) symmetry breaking effects are taken into account

following the prescription of Faessler *et al.* [62] and Schlumpf [61]. We observe that at low  $\bar{\nu}_\tau$  energies, for example at  $E_{\bar{\nu}_\tau} = 4$  GeV, there is some effect of SU(3) symmetry breaking on the  $\frac{d\sigma}{dQ^2}$  if the parametrization by Schlumpf [61] is used, while there is almost no effect if one uses the parametrization of Faessler *et al.* [62]. Moreover, with the increase in  $\bar{\nu}_\tau$  energy, the difference in  $\frac{d\sigma}{dQ^2}$  due to the use of the parametrization of SU(3) symmetry breaking becomes almost negligible. In the case of  $P_L(Q^2)$  and  $P_P(Q^2)$ , the SU(3) symmetry breaking effect is small and is in the range of 1%–2% using Faessler’s model [62] and in the range of 4%–8% using Schlumpf’s model [61] at  $E_{\bar{\nu}_\tau} = 4$  GeV, which becomes even smaller as  $E_{\bar{\nu}_\tau}$  is increased.

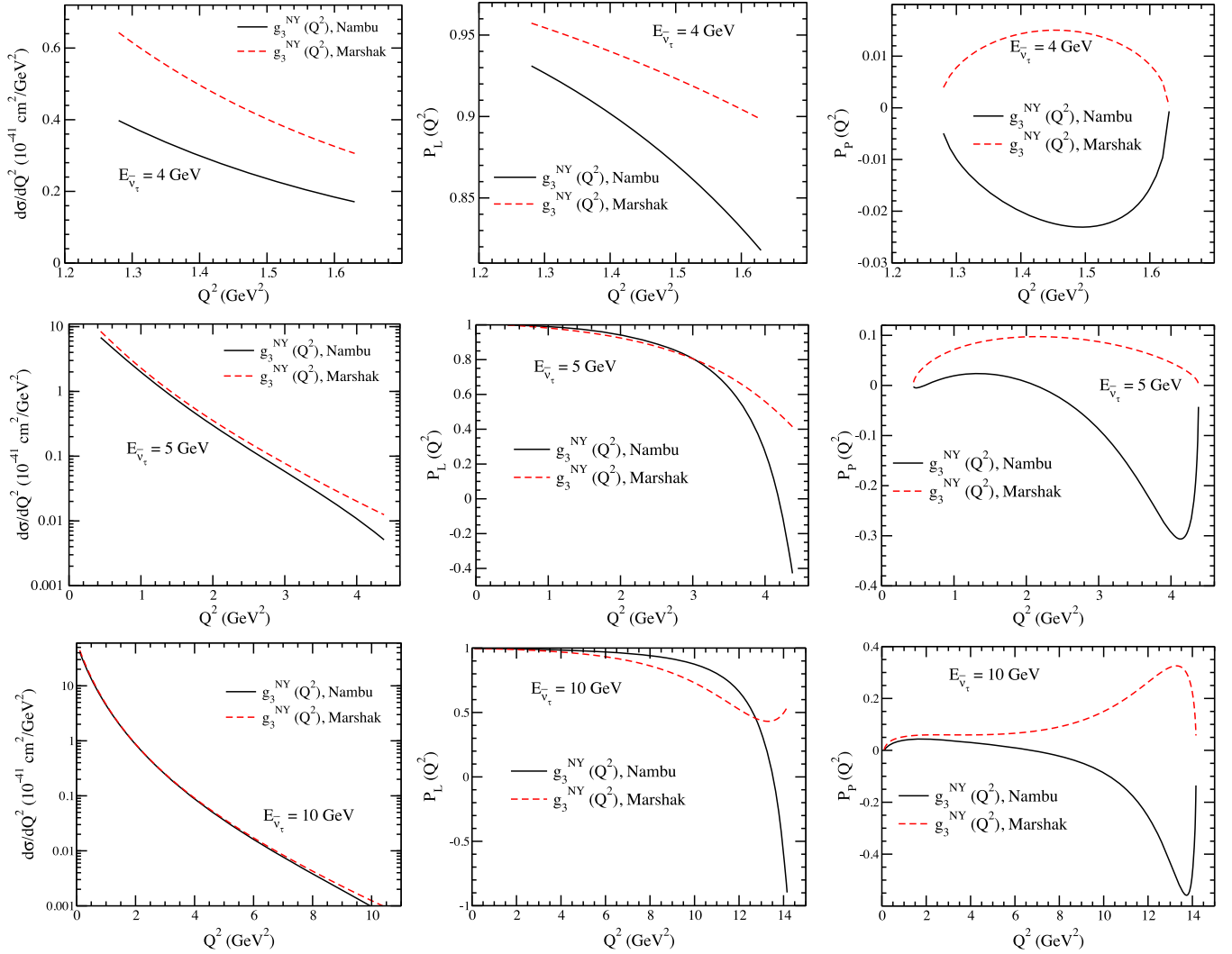


FIG. 5.  $\frac{d\sigma}{dQ^2}$  (left panel),  $P_L(Q^2)$  (middle panel) and  $P_P(Q^2)$  (right panel) versus  $Q^2$  for the process  $\bar{\nu}_\tau + p \rightarrow \tau^+ + \Lambda$  at  $E_{\bar{\nu}_\tau} = 4$  GeV (upper panel), 5 GeV (middle panel), and 10 GeV (lower panel). The calculations have been performed using the SU(3) symmetry with the electric and magnetic Sachs form factors parametrized by Bradford *et al.* [67],  $M_A = 1.026$  GeV, and for the different parametrizations of the pseudoscalar scalar form factor, viz. the parametrizations given by Nambu [77] (solid line) and by Marshak *et al.* [64] (dashed line).

## 2. $\Sigma^-$ production

In Fig. 7 we present the results for  $\frac{d\sigma}{dQ^2}$ ,  $P_L(Q^2)$  and  $P_P(Q^2)$  vs  $Q^2$  for the process  $\bar{\nu}_\tau + n \rightarrow \tau^+ + \Sigma^-$  at the two different values of energies viz.  $E_{\bar{\nu}_\tau} = 5$  GeV and 10 GeV, using the different parametrizations of the nucleon vector form factors viz. BBBA05 [67], Alberico [70], Bosted [68], Galster [72], and Kelly [71]. We observe that at low  $\bar{\nu}_\tau$  energies, for example at  $E_{\bar{\nu}_\tau} = 5$  GeV, there is considerable dependence of the different parametrizations of the vector form factors on  $\frac{d\sigma}{dQ^2}$ ,  $P_L(Q^2)$ , and  $P_P(Q^2)$  distributions. However, unlike the case of  $\Lambda$  production (Fig. 4), with the increase in  $\bar{\nu}_\tau$  energy, this difference further increases and becomes quite significant at higher energies, especially for the distributions of the polarization observables  $P_L(Q^2)$  and  $P_P(Q^2)$ .

The effect of  $M_A$  variation on the differential cross section and polarization observables are presented in Fig. 8, at  $E_{\bar{\nu}_\tau} = 5$  GeV and 10 GeV by varying  $M_A$  in the range 0.9 GeV–1.3 GeV. We find that at low  $\bar{\nu}_\tau$  energies, there is large dependence of these distributions on the choice of  $M_A$ , which increases with an increase in antineutrino energy. It should be noted that in the case of  $\Lambda$  production (Fig. 4), the variation of  $M_A$  on the differential scattering cross section is quite different as compared to the  $M_A$  variation in  $\Sigma^-$  production. This difference arises due to the different parametric form of the axial-vector form factor  $g_1^{NY}(Q^2)$  for  $p \rightarrow \Lambda$  [Eq. (19)] and  $n \rightarrow \Sigma^-$  [Eq. (19)] transitions.

A comparative study of the results presented in Figs. 3–5 for  $\Lambda$  production and in Figs. 7 and 8 for  $\Sigma^-$  production shows that the  $Q^2$  dependence as well as the energy

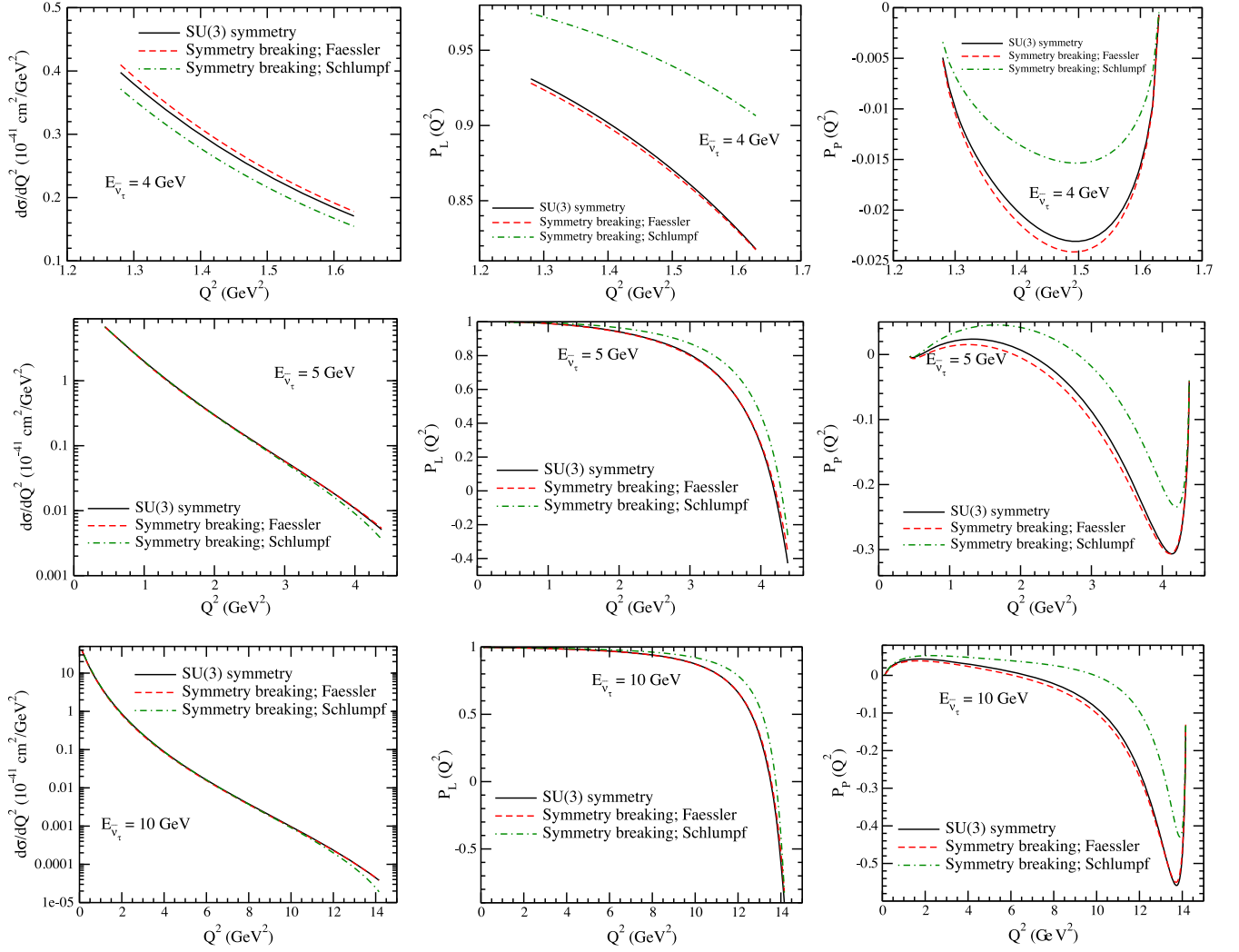


FIG. 6.  $\frac{d\sigma}{dQ^2}$  (left panel),  $P_L(Q^2)$  (middle panel) and  $P_P(Q^2)$  (right panel) versus  $Q^2$  for the process  $\bar{\nu}_\tau + p \rightarrow \tau^+ + \Lambda$  at  $E_{\bar{\nu}_\tau} = 4$  GeV (upper panel), 5 GeV (middle panel), and 10 GeV (lower panel). The calculations have been performed with  $M_A = 1.026$  GeV and BBBA05 [67] for the vector form factors with SU(3) symmetry (solid line), SU(3) symmetry breaking effects parametrized by Faessler *et al.* [62] (dashed line) and the symmetry breaking effects parametrized by Schlumpf [61] (dashed-dotted line).

dependence of the differential cross section  $\frac{d\sigma}{dQ^2}$  are different in the two cases. These differences arise mainly due to the different vector [see Eqs. (14)–(16)] and axial-vector form factors [see Eqs. (19)–(21)] appearing in these cases. Moreover, in the case of  $\Sigma^-$  production, the electromagnetic form factor of the neutron also contributes, unlike the  $\Lambda$  production. The above structure of the matrix elements and their dependence on the form factors leads to different  $Q^2$  and energy behavior in production of these two hyperons.

In Fig. 9 we show the effect of SU(3) symmetry breaking by taking into account the parametrizations given by Faessler *et al.* [62] and Schlumpf [61] on  $\frac{d\sigma}{dQ^2}$ ,  $P_L(Q^2)$  and  $P_P(Q^2)$  vs  $Q^2$  at  $E_{\bar{\nu}_\tau} = 5$  GeV and 10 GeV. From the figure it may be observed that in the case of  $\frac{d\sigma}{dQ^2}$ , the effect of SU(3) symmetry breaking is quite small. However,  $P_L(Q^2)$

shows small effect of SU(3) symmetry breaking, which is about 8% using the parametrization of Faessler *et al.* [62] and  $\sim 10\%$  using the parametrization of Schlumpf [61] at  $E_{\bar{\nu}_\tau} = 5$  GeV, and becomes even smaller with an increase in  $E_{\bar{\nu}_\tau}$ , whereas  $P_P(Q^2)$  shows a small change (1%–2%) when the SU(3) symmetry breaking effects are taken into account.

## B. Total scattering cross section and average polarizations

To study the dependence of the total scattering cross section  $\sigma(E_{\bar{\nu}_\tau})$  and the average polarizations  $P_{L,P}(E_{\bar{\nu}_\tau})$  on  $E_{\bar{\nu}_\tau}$ , we have integrated  $d\sigma/dQ^2$  and  $P_{L,P}(Q^2)$  over  $Q^2$ , and obtained the expressions for  $\sigma(E_{\bar{\nu}_\tau})$  and  $P_{L,P}(E_{\bar{\nu}_\tau})$  i.e.,

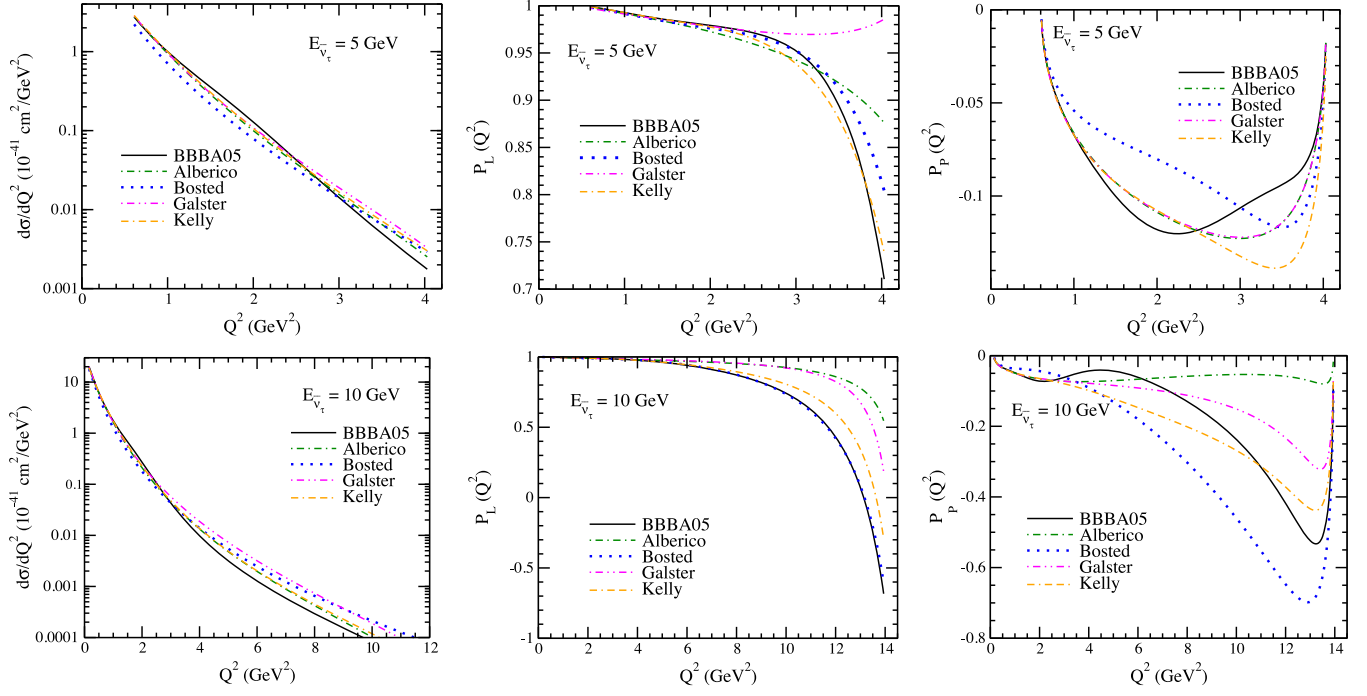


FIG. 7.  $\frac{d\sigma}{dQ^2}$  (left panel),  $P_L(Q^2)$  (middle panel) and  $P_P(Q^2)$  (right panel) versus  $Q^2$  for the process  $\bar{\nu}_\tau + n \rightarrow \tau^+ + \Sigma^-$  at  $E_{\bar{\nu}_\tau} = 5 \text{ GeV}$  (upper panel) and  $10 \text{ GeV}$  (lower panel). The calculations have been performed using the SU(3) symmetry with the axial dipole mass  $M_A = 1.026 \text{ GeV}$  and for the different parametrizations of the nucleon vector form factors viz. BBBA05 [67] (solid line), Alberico *et al.* [70] (dashed-dotted line), Bosted [68] (dotted line), Galster *et al.* [72], (double-dotted-dashed line) and Kelly [71] (double-dashed-dotted line).

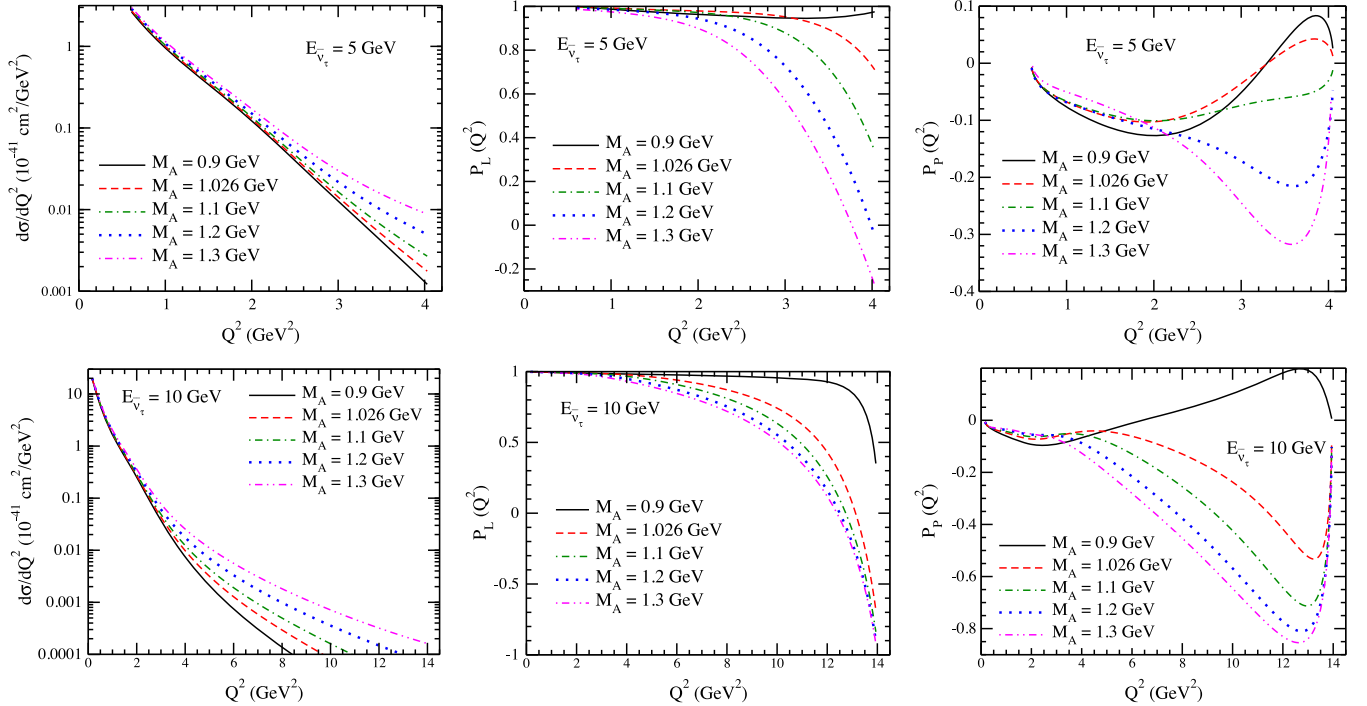


FIG. 8.  $\frac{d\sigma}{dQ^2}$  (left panel),  $P_L(Q^2)$  (middle panel) and  $P_P(Q^2)$  (right panel) versus  $Q^2$  for the process  $\bar{\nu}_\tau + n \rightarrow \tau^+ + \Sigma^-$  at  $E_{\bar{\nu}_\tau} = 5 \text{ GeV}$  (upper panel) and  $10 \text{ GeV}$  (lower panel). The calculations have been performed using the SU(3) symmetry with the electric and magnetic Sachs form factors parametrized by Bradford *et al.* [67] and for the axial form factor, the different values of  $M_A$  have been used viz.  $M_A = 0.9 \text{ GeV}$  (solid line),  $1.026 \text{ GeV}$  (dashed line),  $1.1 \text{ GeV}$  (dashed-dotted line),  $1.2 \text{ GeV}$  (dotted line), and  $1.3 \text{ GeV}$  (double-dotted-dashed line).

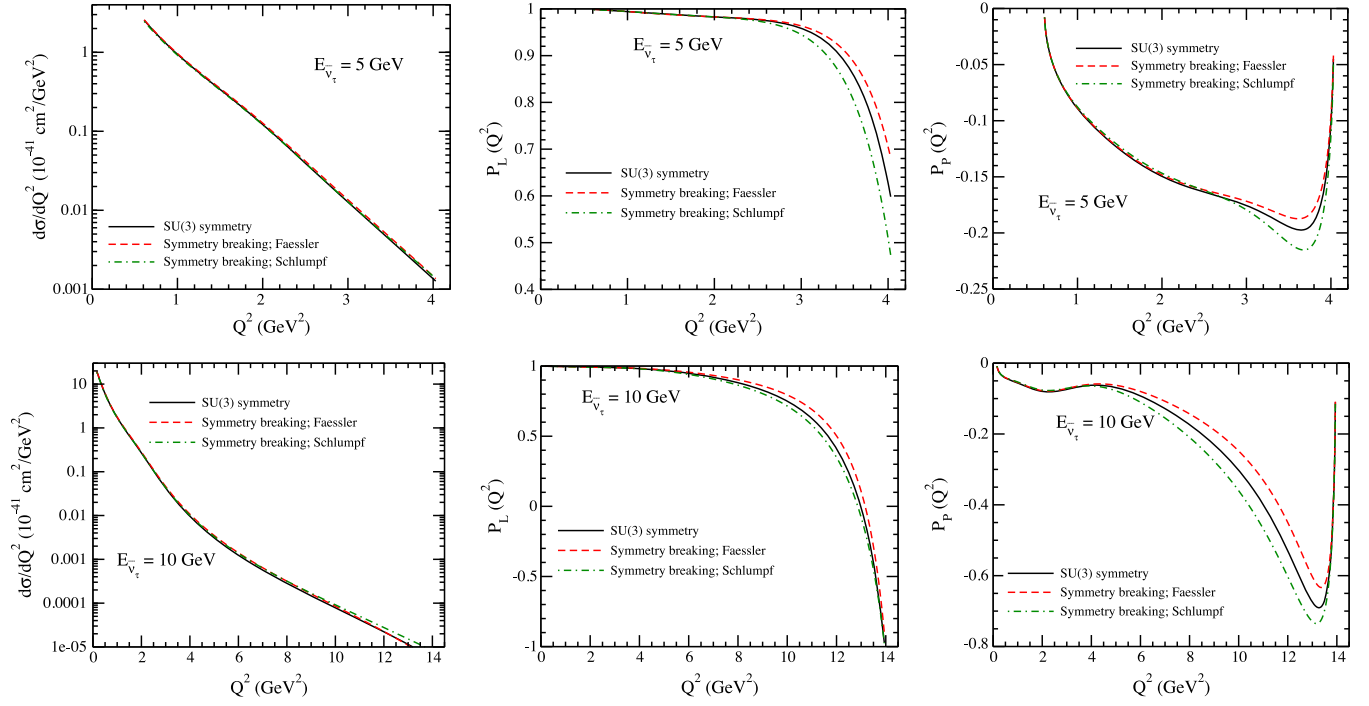


FIG. 9.  $\frac{d\sigma}{dQ^2}$  (left panel),  $P_L(Q^2)$  (middle panel), and  $P_P(Q^2)$  (right panel) versus  $Q^2$  for the process  $\bar{\nu}_\tau + n \rightarrow \tau^+ + \Sigma^-$  at  $E_{\bar{\nu}_\tau} = 5$  GeV (upper panel) and 10 GeV (lower panel). The calculations have been performed with  $M_A = 1.026$  GeV assuming SU(3) symmetry (solid line), as well as with SU(3) symmetry breaking effects parametrized by Faessler *et al.* [62] (dashed line), and by Schlumpf [61] (dashed-dotted line).

$$\sigma(E_{\bar{\nu}_\tau}) = \int_{Q_{\min}^2}^{Q_{\max}^2} \frac{d\sigma}{dQ^2} dQ^2, \quad (50)$$

$$P_{L,P}(E_{\bar{\nu}_\tau}) = \frac{\int_{Q_{\min}^2}^{Q_{\max}^2} P_{L,P}(Q^2) \frac{d\sigma}{dQ^2} dQ^2}{\int_{Q_{\min}^2}^{Q_{\max}^2} \frac{d\sigma}{dQ^2} dQ^2}. \quad (51)$$

In this section we present the results for the total cross section [Eq. (50)] and average polarizations [Eq. (51)] of the tau lepton produced in  $\bar{\nu}_\tau + N \rightarrow \tau^+ + Y$  processes, separately for  $\Lambda$  and  $\Sigma^-$  productions, in Secs. IV B 1 and IV B 2, respectively. This work focuses on  $\bar{\nu}_\tau$  interactions in the GeV energy region in which quasielastic induced reactions make significant contribution. With the increase in antineutrino energy, the inelastic and deep inelastic scattering induced reactions start dominating the total lepton production. In the region of antineutrino energy  $E_{\bar{\nu}_\tau} > 10$  GeV, the quasielastic contribution becomes small [90] and becomes almost negligible as compared to DIS around  $E_{\bar{\nu}_\tau} \sim 100$  GeV, relevant for the future experiments like FASER $\nu$  [16] and SHiP [9–11].

### 1. $\Lambda$ production

In Fig. 10 the results are presented for  $\sigma$  as well as for  $P_L(E_{\bar{\nu}_\tau})$  and  $P_P(E_{\bar{\nu}_\tau})$  obtained using the different values of  $M_A$  viz.  $M_A = 0.9, 1.026, 1.1, 1.2,$  and  $1.3$  GeV for the

process  $\bar{\nu}_\tau + p \rightarrow \tau^+ + \Lambda$ . As expected,  $\sigma$  increases with the increase in antineutrino energy as well as it increases in magnitude with higher values of  $M_A$ . For example, at  $E_{\bar{\nu}_\tau} = 10$  GeV,  $\sigma$  increases by about 25%, when the value of  $M_A$  is increased from its world average value ( $M_A = 1.026$  GeV) by 30% and a decrease in the value of  $M_A$  by 10% from the world average value, decreases the cross section by  $\sim 7\%$ . At low antineutrino energies  $E_{\bar{\nu}_\tau} = 4$  GeV,  $P_L(E_{\bar{\nu}_\tau})$  increases with the increase in  $M_A$ , which is almost 40% when  $M_A$  is varied from 0.9 GeV to 1.3 GeV. However, with the increase in  $E_{\bar{\nu}_\tau}$ , this variation in  $P_L(E_{\bar{\nu}_\tau})$  decreases and becomes almost negligible at  $E_{\bar{\nu}_\tau} = 10$  GeV. We observe some dependence of  $M_A$  on  $P_P(E_{\bar{\nu}_\tau})$  in the entire range of  $E_{\bar{\nu}_\tau}$ . Note that in the case of  $\Lambda$  production,  $\sigma$ ,  $P_L(E_{\bar{\nu}_\tau})$ , and  $P_P(E_{\bar{\nu}_\tau})$  are almost insensitive to the different parametrizations of the Sachs' form factors, and are not shown here explicitly.

In Fig. 11 we show the dependence of  $\sigma$  and  $P_{L,P}(E_{\bar{\nu}_\tau})$  on the pseudoscalar form factor, when the parametrizations by Marshak *et al.* [64] and Nambu [77] are used in the numerical calculations. It may be observed from the figure that  $\sigma$ , as well as the average polarizations, show some dependence on the pseudoscalar form factor.

In Fig. 12 we present the results for  $\sigma$ ,  $P_L(E_{\bar{\nu}_\tau})$  and  $P_P(E_{\bar{\nu}_\tau})$  with SU(3) symmetry as well as when the SU(3) symmetry breaking effects are taken into account following

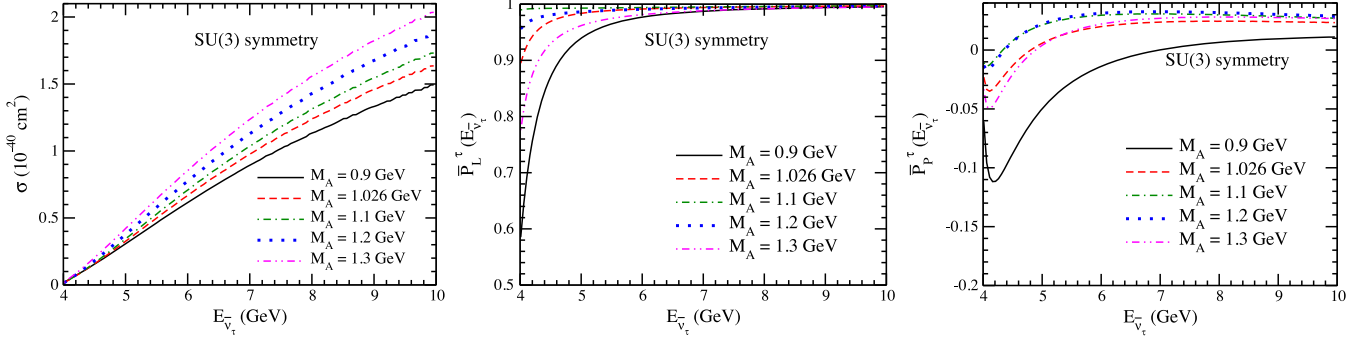


FIG. 10.  $\sigma$  (left panel),  $P_L(E_{\bar{\nu}_\tau})$  (middle panel), and  $P_P(E_{\bar{\nu}_\tau})$  (right panel) vs  $E_{\bar{\nu}_\tau}$  for  $\bar{\nu}_\tau + p \rightarrow \tau^+ + \Lambda$  process. The calculations have been performed using the SU(3) symmetry with electric and magnetic Sachs form factors parametrized by Bradford *et al.* [67] and for the axial form factor, the different values of  $M_A$  have been used viz.  $M_A = 0.9$  GeV (solid line), 1.026 GeV (dashed line), 1.1 GeV (dotted line), 1.2 GeV (dotted line), and 1.3 GeV (double-dotted line).

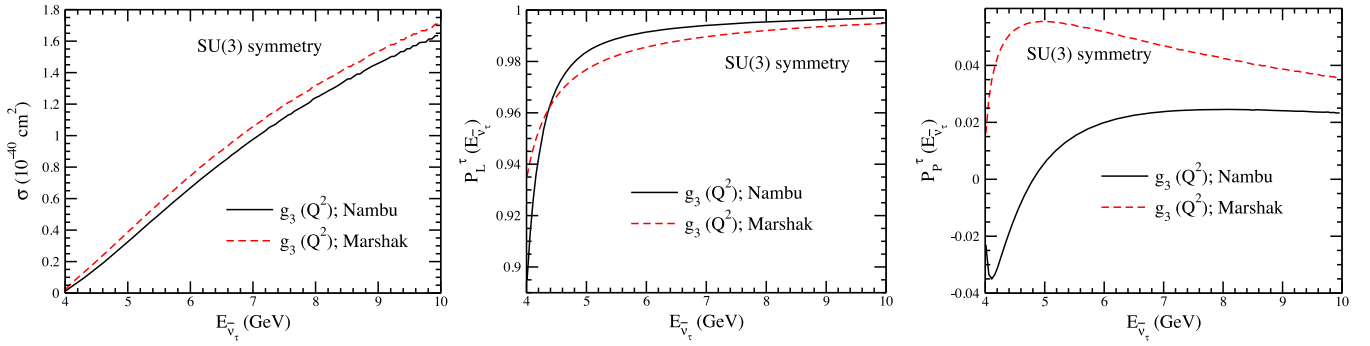


FIG. 11.  $\sigma$  (left panel),  $P_L(E_{\bar{\nu}_\tau})$  (middle panel), and  $P_P(E_{\bar{\nu}_\tau})$  (right panel) vs  $E_{\bar{\nu}_\tau}$  for  $\bar{\nu}_\tau + p \rightarrow \tau^+ + \Lambda$  process. The calculations have been performed using the SU(3) symmetry with electric and magnetic Sachs form factors parametrized by Bradford *et al.* [67] and for the axial form factor,  $M_A = 1.026$  GeV is used, with the different parametrizations of the pseudoscalar form factor viz. using the parametrizations given by Nambu [77] (solid line) and Marshak *et al.* [64] (dashed line).

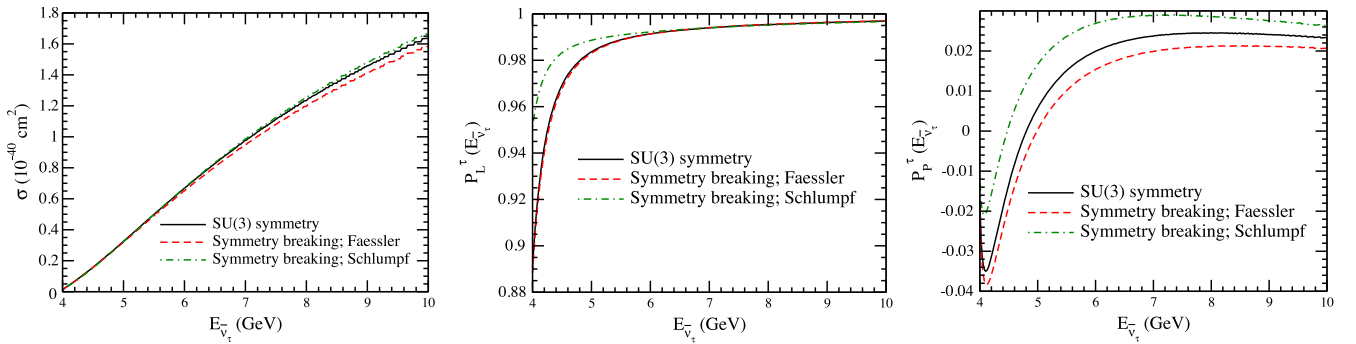


FIG. 12.  $\sigma$  (left panel),  $P_L(E_{\bar{\nu}_\tau})$  (middle panel), and  $P_P(E_{\bar{\nu}_\tau})$  (right panel) vs  $E_{\bar{\nu}_\tau}$  for  $\bar{\nu}_\tau + p \rightarrow \tau^+ + \Lambda$  process. The calculations have been performed using the SU(3) symmetry (solid line), the SU(3) symmetry breaking effects parametrized by Faessler *et al.* [62] (dashed line) and by Schlumpf [61] (dashed-dotted line), with electric and magnetic Sachs form factors parametrized by Bradford *et al.* [67] and for the axial form factor,  $M_A = 1.026$  GeV is used.

the prescriptions of Faessler *et al.* [62] and Schlumpf [61]. We find that there is not much effect of SU(3) symmetry breaking on  $\sigma$ , while there is some effect on  $P_L(E_{\bar{\nu}_\tau})$  whereas in the case of  $P_P(E_{\bar{\nu}_\tau})$ , the effect is found to be significant.

## 2. $\Sigma^-$ production

The dependence of the total cross section and the average polarizations on  $M_A$  are shown in Fig. 13, where we present the results for  $\sigma$  and  $P_{L,P}(E_{\bar{\nu}_\tau})$  for the process  $\bar{\nu}_\tau + n \rightarrow \tau^+ + \Sigma^-$  by varying  $M_A$  in the range,  $M_A = 0.9$  GeV to

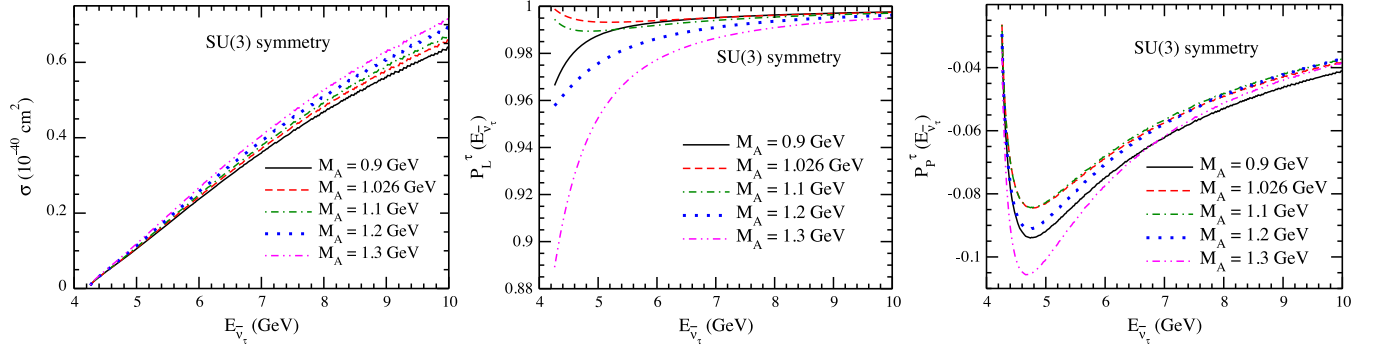


FIG. 13.  $\sigma$  (left panel),  $P_L(E_{\bar{\nu}_\tau})$  (middle panel), and  $P_p(E_{\bar{\nu}_\tau})$  (right panel) vs  $E_{\bar{\nu}_\tau}$  for  $\bar{\nu}_\tau + n \rightarrow \tau^+ + \Sigma^-$  process. The calculations have been performed using the SU(3) symmetry with the electric and magnetic Sachs form factors parametrized by Bradford *et al.* [67] and for the axial form factor, the different values of  $M_A$  have been used viz.  $M_A = 0.9$  GeV (solid line), 1.026 GeV (dashed line), 1.1 GeV (dashed-dotted line), 1.2 GeV (dotted line), and 1.3 GeV (double-dotted-dashed line).

1.3 GeV. The results are qualitatively similar to the results obtained in Fig. 10 for the  $\bar{\nu}_\tau$  induced  $\Lambda$  production.  $\sigma$  increases with increase in the value of  $M_A$  and shows considerable variation at higher antineutrino energies. The average polarizations are quite sensitive to the variation in  $M_A$ , especially at low  $E_{\bar{\nu}_\tau}$ .

In Fig. 14 we show the results for  $\sigma$ ,  $P_L(E_{\bar{\nu}_\tau})$  and  $P_p(E_{\bar{\nu}_\tau})$  with SU(3) symmetry as well as when the SU(3) symmetry breaking effects are taken into account. We find the effect of SU(3) symmetry breaking to be quite small on  $\sigma$  as well as on the polarization observables.

### C. Implications of lepton flavor universality in neutrino scattering

The lepton flavor universality in the  $e - \mu$  sector was proposed long time back in 1947 by Pontecorvo [91] and has been established phenomenologically by studying the weak processes of  $\mu$  decay,  $\mu^-$  capture and  $e^-$  capture from nucleons and nuclei [89]. After the discovery of  $\tau$  lepton and the analyses of its leptonic and semileptonic decays, the principle of lepton flavor universality was extended to the

$e - \mu - \tau$  sector. As mentioned in the introduction in Sec. I, recently there has been considerable work in studying the implications of lepton flavor universality in weak interactions in the  $e - \mu - \tau$  sector, which have focused mainly on the decay processes [30–42]. While there has been very little work on the study of lepton flavor universality in the scattering processes induced by  $\nu_e$ ,  $\nu_\mu$ , and  $\nu_\tau$ . The difference in the  $\nu_e$  and  $\nu_\mu$  cross sections using different nuclear models has been studied by various groups like Refs. [55–59]. The implications of lepton flavor universality in the  $e - \mu$  sector by studying the quasielastic scattering induced by  $\nu_e(\bar{\nu}_e)$  and  $\nu_\mu(\bar{\nu}_\mu)$  have been studied by Day and McFarland [60] for the free nucleons and Akbar *et al.* [55] on nuclear targets. They have reported the results comparing the cross sections of quasielastic scattering of  $\nu_e(\bar{\nu}_e)$  and  $\nu_\mu(\bar{\nu}_\mu)$  with free nucleons [60] and with nuclear targets [55] induced by the  $\Delta S = 0$  weak charged current reactions. In Ref. [60], Day and McFarland have assumed the LFU and studied the differences in the electron and muon production cross section arising due to the lepton mass effect and other effects that depend upon the lepton

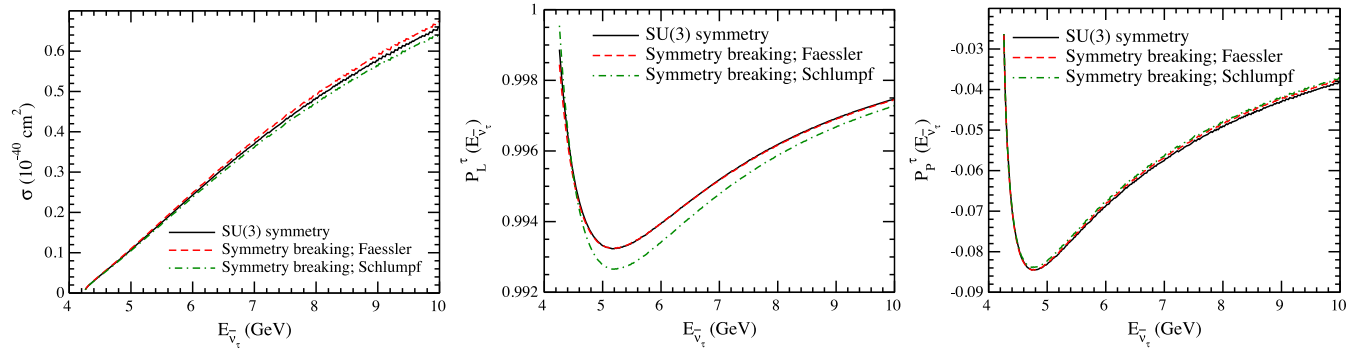


FIG. 14.  $\sigma$  (left panel),  $P_L(E_{\bar{\nu}_\tau})$  (middle panel), and  $P_p(E_{\bar{\nu}_\tau})$  (right panel) vs  $E_{\bar{\nu}_\tau}$  for  $\bar{\nu}_\tau + n \rightarrow \tau^+ + \Sigma^-$  process. The calculations have been performed using the SU(3) symmetry (solid line), the SU(3) symmetry breaking effects parametrized by Faessler *et al.* [62] (dashed line) and by Schlumpf [61] (dashed-dotted line), with electric and magnetic Sachs form factors parametrized by Bradford *et al.* [67] and for the axial form factor,  $M_A = 1.026$  GeV is used.

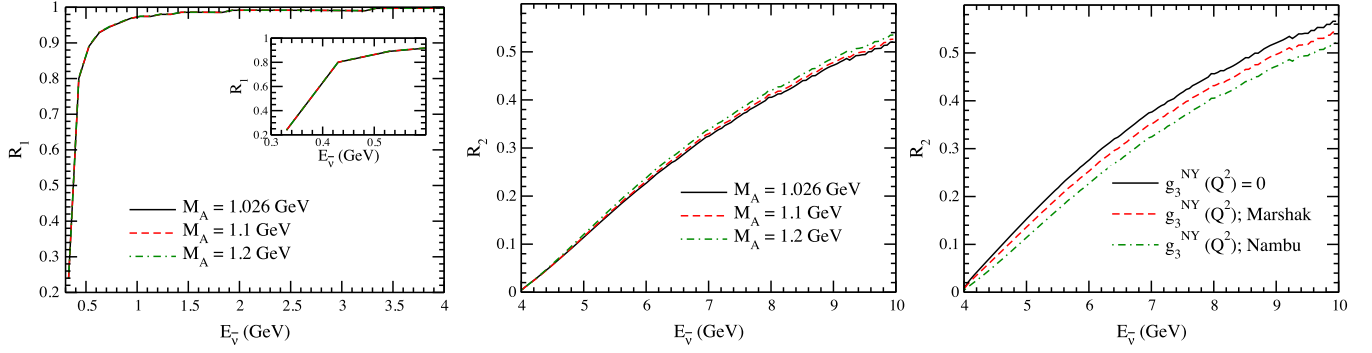


FIG. 15.  $R_1$  as a function of  $E_{\bar{\nu}}$  (left panel) with  $M_A = 1.026$  GeV (solid line),  $M_A = 1.1$  GeV (dashed line) and  $M_A = 1.2$  GeV (dashed-dotted line).  $R_2$  as a function of  $E_{\bar{\nu}}$  (middle panel) with  $M_A = 1.026$  GeV (solid line),  $M_A = 1.1$  GeV (dashed line), and  $M_A = 1.2$  GeV (dashed-dotted line).  $R_2$  as a function of  $E_{\bar{\nu}}$  (right panel) with  $g_3^{NY}(Q^2) = 0$  (solid line), the parametrization of  $g_3^{NY}(Q^2)$  by Marshak *et al.* [64] (dashed line) and by Nambu [77] (dashed-dotted line).

mass like the radiative corrections, the pseudoscalar form factor as well as the form factors associated with the second class currents. In Ref. [55], Akbar *et al.* have studied these differences in the neutrino-nucleon cross sections including the nuclear medium effects, which are important in the intermediate energy region where most of the present neutrino experiments are being done.

In this section we study the implications of LFU in the  $\Delta S = 1$  sector of antineutrino scattering, and compare the total cross sections for  $e$ ,  $\mu$  and  $\tau$  productions in the quasielastic scattering of  $\bar{\nu}_e$ ,  $\bar{\nu}_\mu$ , and  $\bar{\nu}_\tau$  from the nucleons induced by the weak charged currents. Specifically, we study the ratios of the total cross sections  $R_1$  and  $R_2$ , defined as

$$R_1 = \frac{\sigma(\bar{\nu}_\mu + p \rightarrow \mu^+ + \Lambda)}{\sigma(\bar{\nu}_e + p \rightarrow e^+ + \Lambda)}, \quad (52)$$

$$R_2 = \frac{2\sigma(\bar{\nu}_\tau + p \rightarrow \tau^+ + \Lambda)}{\sigma(\bar{\nu}_\mu + p \rightarrow \mu^+ + \Lambda) + \sigma(\bar{\nu}_e + p \rightarrow e^+ + \Lambda)}, \quad (53)$$

as a function of antineutrino energy  $E_{\bar{\nu}}$  and investigate the effect of axial dipole mass  $M_A$  and the pseudoscalar form factor  $g_3^{NY}(Q^2)$  assuming the SU(3) symmetry. The numerical results are calculated by taking  $M_A = 1.026$  GeV and the parametrization of  $g_3^{NY}(Q^2)$  by Nambu, unless stated otherwise, and presented in Fig. 15. We have also studied the effect of changing the vector form factors as well as the effect of SU(3) symmetry breaking. These effects are found to be quantitatively very small on  $R_1(E_{\bar{\nu}})$  and  $R_2(E_{\bar{\nu}})$ , and are not presented here.

We see from Fig. 15 that

- (i) the ratios  $R_1(E_{\bar{\nu}})$  (Eq. (52)) and  $R_2(E_{\bar{\nu}})$  (Eq. (53)) have very little dependence on the choice of  $M_A$ , which is almost negligible in the case of  $R_1(E_{\bar{\nu}})$ . It may be noticed that in the kinematic region of  $\tau$

production i.e.,  $E_{\bar{\nu}} \simeq 4$  GeV, the ratio  $R_1(E_{\bar{\nu}})$  is almost unity. While in the case of  $R_2(E_{\bar{\nu}})$ , the ratio is highly suppressed due to the threshold effects and becomes more than 0.5, only for  $E_{\bar{\nu}} > 10$  GeV. Thus, any deviation of  $R_1(E_{\bar{\nu}})$  and  $R_2(E_{\bar{\nu}})$  from the values shown in Fig. 15, would be a possible signal for the violation of LFU.

- (ii) the ratio  $R_2(E_{\bar{\nu}})$  has some dependence on the choice of the pseudoscalar form factor  $g_3^{NY}(Q^2)$ . If we take  $g_3^{NY}(Q^2) = 0$  or the parametrization of  $g_3^{NY}(Q^2)$  given by Marshak *et al.* [64], the value of  $R_2(E_{\bar{\nu}})$  increases as compared to the value obtained by using the parametrization of  $g_3^{NY}(Q^2)$  given by Nambu [77]. For example, at  $E_{\bar{\nu}} = 10$  GeV, when we compare the results obtained with  $g_3^{NY}(Q^2)$  using the parametrization of Marshak *et al.* [64], the value of  $R_2(E_{\bar{\nu}})$  increases by 5%, which becomes 18% at  $E_{\bar{\nu}} = 5$  GeV, from the results obtained using  $g_3^{NY}(Q^2)$  parametrized by Marshak *et al.* [64]. Therefore, an experimental determination of  $R_2(E_{\bar{\nu}})$  with a precision of 20% or higher would be able to show any evidence of the violation of LFU in the  $e - \mu - \tau$  sector.

## V. SUMMARY AND CONCLUSIONS

In this work we have presented the results for the  $|\Delta S| = 1$  hyperon production in the quasielastic  $\bar{\nu}_\tau$ -nucleon scattering and obtained the differential ( $\frac{d\sigma}{dQ^2}$ ) and total ( $\sigma$ ) scattering cross sections as well as the longitudinal ( $P_L$ ) and perpendicular ( $P_P$ ) components of the polarized  $\tau^+$  lepton produced in these reactions. We studied theoretical uncertainties arising due to the use of different vector, axial-vector, and pseudoscalar form factors as well as the effect of SU(3) symmetry breaking on these observables.



Our observations are the following:

- (i) In the case of  $\Lambda$  production, the total cross section as well as the average polarizations increases with increase in  $M_A$  at low antineutrino energies, say at  $E_{\bar{\nu}_\tau} = 5$  GeV. However, with the increase in  $E_{\bar{\nu}_\tau}$ ,  $\sigma$  further increases with  $M_A$  while  $P_{L,P}(E_{\bar{\nu}_\tau})$  saturates with increase in  $M_A$ . Moreover, in the case of  $\Sigma^-$  production, the results for  $\sigma$  as well as  $P_{L,P}(E_{\bar{\nu}_\tau})$  are qualitatively similar to the results obtained for  $\Lambda$  production.
- (ii) There is not much effect of SU(3) symmetry breaking on  $\sigma$  for both  $\Lambda$  and  $\Sigma^-$  productions. However, we observe some dependence of the symmetry breaking effect on  $P_{L,P}(E_{\bar{\nu}_\tau})$ , for  $\Lambda$  production.
- (iii) In the case of  $\Lambda$  production, at low  $\bar{\nu}_\tau$  energies, specifically near the threshold energy, the effect of the different parametrizations of vector form factors on  $\frac{d\sigma}{dQ^2}$ ,  $P_L(Q^2)$  and  $P_P(Q^2)$  distributions is large, which decreases with the increase in  $E_{\bar{\nu}_\tau}$ . However, in the case of  $\Sigma^-$  production,  $\frac{d\sigma}{dQ^2}$  shows appreciable dependence on the different parametrizations of the vector form factors for all values of  $E_{\bar{\nu}_\tau}$ , while  $P_L(Q^2)$  and  $P_P(Q^2)$  distributions are quite sensitive to the choice of the vector form factors.
- (iv) The effect of variation in the axial dipole mass  $M_A$  on  $\frac{d\sigma}{dQ^2}$ ,  $P_L(Q^2)$  and  $P_P(Q^2)$ , when  $\Lambda$  is produced in the final state, is significant at low  $E_{\bar{\nu}_\tau}$ , which decreases with the increase in  $E_{\bar{\nu}_\tau}$  for  $Q^2$  and  $P_L(Q^2)$  distributions but for  $P_P(Q^2)$  distribution still remains significantly different even at high  $\bar{\nu}_\tau$  energies. While there is a large dependence of  $M_A$  on  $\frac{d\sigma}{dQ^2}$ ,  $P_L(Q^2)$  and  $P_P(Q^2)$  at all values of  $Q^2$  and  $E_{\bar{\nu}_\tau}$ , when  $\Sigma^-$  is produced in the final state.
- (v) In the case of  $\Lambda$  production, the effect of SU(3) symmetry breaking on  $\frac{d\sigma}{dQ^2}$  is very small at all values of  $E_{\bar{\nu}_\tau}$  and  $Q^2$  while there is a sizeable effect of SU(3) symmetry breaking on  $P_L(Q^2)$  and  $P_P(Q^2)$ . However, in the case of  $\Sigma^-$  production, the effect of SU(3) symmetry breaking on  $\frac{d\sigma}{dQ^2}$  is small at low  $E_{\bar{\nu}_\tau}$ , and increases with the increase in energy. Moreover, different results for the polarization observables are obtained, though the variation is small, when the SU(3) symmetry breaking using the prescriptions by Schlumpf [61] and Faessler *et al.* [62] are taken into account.
- (vi) We have also tested the lepton flavor universality in the antineutrino induced  $\Lambda$  production by calculating the ratios [given in Eqs. (52) and (53)] of the total cross sections in the  $e - \mu$  and  $e - \mu - \tau$  sectors. We find that there is no dependence of  $M_A$  or the SU(3) symmetry breaking on  $R_1$ . However,  $R_2$  shows some dependence on the choice of  $M_A$  as well as to the different parametrizations of the pseudoscalar form factor. Thus, the experimental observation of  $R_2(E_{\bar{\nu}_\tau})$  with a precision of 20% or higher would be able to show any evidence of the violation of LFU in the  $e - \mu - \tau$  sector.

## ACKNOWLEDGMENTS

A. F. and M. S. A. are thankful to the Department of Science and Technology, Government of India for providing financial assistance under Grant No. SR/MF/PS-01/2016-AMU.

- 
- [1] K. Kodama *et al.* (DONUT Collaboration), *Phys. Lett. B* **504**, 218 (2001).
  - [2] K. Kodama *et al.* (DONUT Collaboration), *Phys. Rev. D* **78**, 052002 (2008).
  - [3] N. Agafonova *et al.* (OPERA Collaboration), *Phys. Rev. D* **89**, 051102 (2014).
  - [4] N. Agafonova *et al.* (OPERA Collaboration), *Phys. Rev. Lett.* **115**, 121802 (2015).
  - [5] N. Agafonova *et al.* (OPERA Collaboration), *Phys. Rev. Lett.* **120**, 211801 (2018).
  - [6] Z. Li *et al.* (Super-Kamiokande Collaboration), *Phys. Rev. D* **98**, 052006 (2018).
  - [7] K. Abe *et al.* (Super-Kamiokande Collaboration), *Phys. Rev. Lett.* **110**, 181802 (2013).
  - [8] M. G. Aartsen *et al.* (IceCube Collaboration), *Phys. Rev. D* **99**, 032007 (2019).
  - [9] C. Yoon (SHiP Collaboration), *Proc. Sci., NuFact2019* (2020) 103.
  - [10] M. Anelli *et al.* (SHiP Collaboration), *arXiv:1504.04956*.
  - [11] S. Alekhin *et al.*, *Rep. Prog. Phys.* **79**, 124201 (2016).
  - [12] S. Aoki *et al.* (DsTau Collaboration), *J. High Energy Phys.* **01** (2020) 033.
  - [13] P. Machado, H. Schulz, and J. Turner, *Phys. Rev. D* **102**, 053010 (2020).
  - [14] J. Strait *et al.* (DUNE Collaboration), *arXiv:1601.05823*.
  - [15] B. Abi *et al.* (DUNE Collaboration), *arXiv:1807.10340*.
  - [16] H. Abreu *et al.* (FASER Collaboration), *arXiv:2001.03073*.
  - [17] A. Fatima, M. Sajjad Athar, and S. K. Singh, *Phys. Rev. D* **102**, 113009 (2020).
  - [18] K. S. Kuzmin, V. V. Lyubushkin, and V. A. Naumov, *Mod. Phys. Lett. A* **19**, 2815 (2004); *Phys. Part. Nucl.* **35**, S133 (2004).
  - [19] K. S. Kuzmin, V. V. Lyubushkin, and V. A. Naumov, *Mod. Phys. Lett. A* **19**, 2919 (2004).
  - [20] K. Hagiwara, K. Mawatari, and H. Yokoya, *Nucl. Phys.* **B668**, 364 (2003).

- [21] K. Hagiwara, K. Mawatari, and H. Yokoya, *Nucl. Phys. B, Proc. Suppl.* **139**, 140 (2005).
- [22] K. Hagiwara, K. Mawatari, and H. Yokoya, *Phys. Lett. B* **591**, 113 (2004).
- [23] J. E. Sobczyk, N. Rocco, and J. Nieves, *Phys. Rev. C* **100**, 035501 (2019).
- [24] M. Valverde, J. E. Amaro, J. Nieves, and C. Maieron, *Phys. Lett. B* **642**, 218 (2006).
- [25] A. Fatima, M. Sajjad Athar, and S. K. Singh, *Eur. Phys. J. A* **54**, 95 (2018).
- [26] A. Fatima, M. Sajjad Athar, and S. K. Singh, *Phys. Rev. D* **98**, 033005 (2018).
- [27] A. Fatima, M. Sajjad Athar, and S. K. Singh, *Front. Phys.* **7**, 13 (2019).
- [28] A. Fatima, M. Sajjad Athar, and S. K. Singh, *Eur. Phys. J. Special Topics* **230**, 4391 (2021).
- [29] G. Aad *et al.* (ATLAS Collaboration), *Nat. Phys.* **17**, 813 (2021).
- [30] S. F. Zhang (BESIII Collaboration), arXiv:1906.08912.
- [31] Y. H. Yang (BESIII Collaboration), arXiv:1812.00320.
- [32] R. Fleischer, R. Jaarsma, and G. Koole, *Eur. Phys. J. C* **80**, 153 (2020).
- [33] M. Golz, *Proc. Sci., CHARM2020* (2021) 051.
- [34] M. Ablikim *et al.* (BESIII Collaboration), *Phys. Rev. Lett.* **127**, 121802 (2021).
- [35] M. Ablikim *et al.* (BESIII Collaboration), *Phys. Rev. Lett.* **122**, 011804 (2019).
- [36] G. Mezzadri (BESIII Collaboration), *Proc. Sci., BEAUTY2018* (2018) 025.
- [37] S. Bifani, S. Descotes-Genon, A. Romero Vidal, and M. H. Schune, *J. Phys. G* **46**, 023001 (2019).
- [38] J. Albrecht, D. van Dyk, and C. Langenbruch, *Prog. Part. Nucl. Phys.* **120**, 103885 (2021).
- [39] R. Aaij *et al.* (LHCb Collaboration), *Nat. Phys.* **18**, 277 (2022).
- [40] P. de Simone (LHCb Collaboration), *EPJ Web Conf.* **234**, 01004 (2020).
- [41] G. Caria *et al.* (Belle Collaboration), *Phys. Rev. Lett.* **124**, 161803 (2020).
- [42] S. Celani (LHCb Collaboration), arXiv:2111.11105.
- [43] A. Crivellin and M. Hoferichter, *Science* **374**, 1051 (2021).
- [44] D. Bryman, V. Cirigliano, A. Crivellin, and G. Inguglia, arXiv:2111.05338.
- [45] B. Abi *et al.* (Muon  $g-2$  Collaboration), *Phys. Rev. Lett.* **126**, 141801 (2021).
- [46] A. M. Coutinho, A. Crivellin, and C. A. Manzari, *Phys. Rev. Lett.* **125**, 071802 (2020).
- [47] A. M. Sirunyan *et al.* (CMS Collaboration), *J. High Energy Phys.* **07** (2021) 208.
- [48] L. Allwicher, G. Isidori, and N. Selimovic, *Phys. Lett. B* **826**, 136903 (2022).
- [49] A. Crivellin, M. Hoferichter, M. Kirk, C. A. Manzari, and L. Schnell, *J. High Energy Phys.* **10** (2021) 221.
- [50] D. London and J. Matias, arXiv:2110.13270.
- [51] L. Zhang, X. W. Kang, X. H. Guo, L. Y. Dai, T. Luo, and C. Wang, *J. High Energy Phys.* **02** (2021) 179.
- [52] D. Bečirević, F. Jaffredo, A. Peñuelas, and O. Sumensari, *J. High Energy Phys.* **05** (2021) 175.
- [53] X. Leng, X. L. Mu, Z. T. Zou, and Y. Li, *Chin. Phys. C* **45**, 063107 (2021).
- [54] S. Zhang (BESIII Collaboration), *SciPost Phys. Proc.* **1**, 016 (2019).
- [55] F. Akbar, M. Rafi Alam, M. Sajjad Athar, S. Chauhan, S. K. Singh, and F. Zaidi, *Int. J. Mod. Phys. E* **24**, 1550079 (2015).
- [56] A. M. Ankowski, *Phys. Rev. C* **96**, 035501 (2017).
- [57] M. Martini, N. Jachowicz, M. Ericson, V. Pandey, T. Van Cuyck, and N. Van Dessel, *Phys. Rev. C* **94**, 015501 (2016).
- [58] J. Nieves and J. E. Sobczyk, *Ann. Phys. (Amsterdam)* **383**, 455 (2017).
- [59] A. Nikolakopoulos, N. Jachowicz, N. Van Dessel, K. Niewczas, R. González-Jiménez, J. M. Udías, and V. Pandey, *Phys. Rev. Lett.* **123**, 052501 (2019).
- [60] M. Day and K. S. McFarland, *Phys. Rev. D* **86**, 053003 (2012).
- [61] F. Schlumpf, *Phys. Rev. D* **51**, 2262 (1995).
- [62] A. Faessler, T. Gutsche, B. R. Holstein, M. A. Ivanov, J. G. Korner, and V. E. Lyubovitskij, *Phys. Rev. D* **78**, 094005 (2008).
- [63] X. G. He, J. Tandean, and G. Valencia, *J. High Energy Phys.* **07** (2019) 022.
- [64] R. E. Marshak, Riazuddin, and C. P. Ryan, *Theory of Weak Interactions in Particle Physics* (Wiley-Interscience, New York, 1969).
- [65] A. Pais, *Ann. Phys. (N.Y.)* **63**, 361 (1971).
- [66] C. H. Llewellyn Smith, *Phys. Rep.* **3**, 261 (1972).
- [67] R. Bradford, A. Bodek, H. Budd, and J. Arrington, *Nucl. Phys.* **159**, 127 (2006).
- [68] P. E. Bosted, *Phys. Rev. C* **51**, 409 (1995).
- [69] H. Budd, A. Bodek, and J. Arrington, *Nucl. Phys.* **139**, 90 (2005).
- [70] W. M. Alberico, S. M. Bilenky, C. Giunti, and K. M. Graczyk, *Phys. Rev. C* **79**, 065204 (2009).
- [71] J. J. Kelly, *Phys. Rev. C* **70**, 068202 (2004).
- [72] S. Galster, H. Klein, J. Moritz, K. H. Schmidt, D. Wegener, and J. Bleckwenn, *Nucl. Phys.* **B32**, 221 (1971).
- [73] S. Platchkov *et al.*, *Nucl. Phys.* **A510**, 740 (1990).
- [74] V. Punjabi, C. F. Perdrisat, M. K. Jones, E. J. Brash, and C. E. Carlson, *Eur. Phys. J. A* **51**, 79 (2015).
- [75] N. Cabibbo, E. C. Swallow, and R. Winston, *Annu. Rev. Nucl. Part. Sci.* **53**, 39 (2003).
- [76] V. Bernard, L. Elouadrhiri, and U. G. Meissner, *J. Phys. G* **28**, R1 (2002).
- [77] Y. Nambu, *Phys. Rev. Lett.* **4**, 380 (1960).
- [78] R. M. Wang, M. Z. Yang, H. B. Li, and X. D. Cheng, *Phys. Rev. D* **100**, 076008 (2019).
- [79] P. E. Shanahan, A. N. Cooke, R. Horsley, Y. Nakamura, P. E. L. Rakow, G. Schierholz, A. W. Thomas, R. D. Young, and J. M. Zanotti, *Phys. Rev. D* **92**, 074029 (2015).
- [80] G. S. Yang and H. C. Kim, *Phys. Rev. C* **92**, 035206 (2015).
- [81] D. Becirevic, D. Guadagnoli, G. Isidori, V. Lubicz, G. Martinelli, F. Mescia, M. Papinutto, S. Simula, C. Tarantino, and G. Villadoro, *Eur. Phys. J. A* **24**, 69 (2005).
- [82] A. Lacour, B. Kubis, and U. G. Meissner, *J. High Energy Phys.* **10** (2007) 083.
- [83] T. N. Pham, *Phys. Rev. D* **87**, 016002 (2013).
- [84] T. N. Pham, *Nucl. Part. Phys. Proc.* **258**, 102 (2015).
- [85] T. Ledwig, J. Martin Camalich, L. S. Geng, and M. J. Vicente Vacas, *Phys. Rev. D* **90**, 054502 (2014).

- [86] H. M. Chang, M. González-Alonso, and J. Martin Camalich, *Phys. Rev. Lett.* **114**, 161802 (2015).
- [87] M. Ademollo and R. Gatto, *Phys. Rev. Lett.* **13**, 264 (1964).
- [88] S. M. Bilenky, *Basics of Introduction to Feynman Diagrams and Electroweak Interactions Physics* (Editions Frontieres, Gif-sur-Yvette Cedex, 1994).
- [89] M. Sajjad Athar and S. K. Singh, *The Physics of Neutrino Interactions* (Cambridge University Press, Cambridge, England, 2020).
- [90] E. A. Paschos and J. Y. Yu, *Phys. Rev. D* **65**, 033002 (2002).
- [91] B. Pontecorvo, *Phys. Rev.* **72**, 246 (1947).